Cover Letter

Dear Editor,

We are truly grateful to the reviewers' critical comments and comprehensive suggestions on our manuscript. Based on these comments and suggestions, we have made significant modifications on the original manuscript. **The whole manuscript has been carefully checked and a lot of paragraphs have been added or rewritten to better the structure. The sections of abstract, discussion, and conclusions are all rewritten. All changes made in the text are marked with red color in the revised manuscript.** The point-to-point responses to the reviewers' comments are listed as below. We hope the revised manuscript is now suitable for publication in ***Atmospheric Chemistry and Physics***. Thank you for your consideration.

Best wishes

Sincerely yours

Prof. Kun Luo (corresponding author)
State Key Laboratory of Clean Energy Utilization,
Zhejiang University, Hangzhou 310027, P. R. China
E-mail: zjulk@zju.edu.cn; Tel/Fax: 86-571-87951764

Style Definition ... [63]
Style Definition ... [62]
Style Definition ... [61]
Style Definition ... [60]
Style Definition ... [59]
Style Definition ... [58]
Style Definition ... [57]
Style Definition ... [56]
Style Definition ... [55]
Style Definition ... [54]
Style Definition ... [53]
Style Definition ... [52]
Style Definition ... [51]
Style Definition ... [50]
Style Definition ... [49]
Style Definition ... [48]
Style Definition ... [47]
Style Definition ... [46]
Style Definition ... [45]
Style Definition ... [44]
Style Definition ... [43]
Style Definition ... [42]
Style Definition ... [41]
Style Definition ... [40]
Style Definition ... [39]
Style Definition ... [38]
Style Definition ... [37]
Style Definition ... [36]
Style Definition ... [35]
Style Definition ... [34]
Style Definition ... [33]
Style Definition ... [32]
Style Definition ... [31]
Style Definition ... [30]
Style Definition ... [29]
Style Definition ... [28]
Style Definition ... [27]
Style Definition ... [26]
Style Definition ... [25]
Style Definition ... [24]
Style Definition ... [23]
Style Definition ... [22]
Style Definition ... [21]
Style Definition ... [20]
Style Definition ... [19]
Style Definition ... [18]
Style Definition ... [17]
Style Definition ... [16]
Style Definition ... [15]
Style Definition ... [14]
Style Definition ... [13]
Style Definition ... [12]
Style Definition ... [11]
Style Definition ... [10]
Style Definition ... [9]
Style Definition ... [8]
Style Definition ... [7]
Style Definition ... [6]
Style Definition ... [5]
Style Definition ... [4]
Style Definition ... [3]
Style Definition ... [2]
Style Definition ... [1]

Replies to reviewers' comments point by point

Referee #1

1. While this is an interesting case study, the motivation of the paper is not clear to me. Specifically, the authors did not say whether [a] they want to study how surface ozone responded to the tropical cyclone during their study period or [b] if they are interested in understanding whether emergency control measures put in place for the G20 meeting helped reduce ozone levels or not? If their objective is [a], this study lacks novelty because it is now well understood that clear-sky stagnant conditions favor photochemical ozone formation and cloudy-skies suppress it. Thus, ozone variations reported and modeled before, during, and after the cyclone are expected and there is no new knowledge gained here. If their objective is [b], the model experimental design is not appropriate. The authors did not modify their emission input to reflect emission control measures in their model simulations and no sensitivity experiment was performed to understand what would have happened in the absence of emergency emission control measures?

Reply: Thank you for this valuable comment. Accordingly, we have highlighted the motivation of the present study by rewriting the introduction with two additional paragraphs. The main objective of the present study is to understand the unique response of ozone increase to emission control measures during the 2016 G20 Summit in Hangzhou, while other pollutants had been significantly reduced (Li et al. 2019; Wu et al. 2019; Ji et al. 2018; Zheng et al. 2019). The title of the manuscript is also changed as "Spatial-temporal Variations and Process Analysis of O3 Pollution in Hangzhou during the G20 Summit" to reflect this motivation. For this purpose, a regional air quality model, within the framework of the Model Inter-Comparison Study for ASIA phase III (Li et al., 2019), is used to investigate the spatial-temporal variations of ozone pollution in Hangzhou during the G20 Summit. Process analysis is conducted to understand the chemical and physical factors that contribute to the local O_3 abundance. It is worth noting that the base emission input has been modified to reflect emission control measures in our model simulations. Sensitivity experiments are not performed as

previous surface observations (Li et al. 2019; Wu et al. 2019; Ji et al. 2018; Zheng et al. 2019) have suggested that the control measures took no immediate effect on local ozone formation, but significantly reduced other pollutants. The added two paragraphs are attached as below.

"Hangzhou, the capital of Zhejiang Province, is located in the center of the Yangtze River Delta which is one of the most developed areas in China. Resultant from local emissions (Wu et al. 2014, Hu et al. 2015) and transboundary transport of aerosol and trace gases transport (Liu et al. 2015; Ni et al. 2018; Zhang et al. 2018), air pollution in Hangzhou has become serious in the recent years. In 2016, Hangzhou city would host the 2016 G20 (Group of Twenty Finance Ministers and Central Bank Governors) summit during September 4-6. To improve air quality for this event, 14-day temporarily strict air pollution alleviation measures had been taken to reduce air pollutant emissions in Hangzhou and surrounding areas from August 24 to September 6, 2016. The emission control scheme includes a coal-fired power plant capacity 50% reduction since August 24, followed by an "odd-even" on-road vehicle restriction since August 28, and further emergent VOC reduction from industrial sectors since September 1 to 6 (Ji et al. 2018; Li et al. 2019; Wu et al. 2019). These short-term measures provide a valuable opportunity to investigate the response of air quality to the emission reduction, understand the formation mechanisms of air pollution, and explore effective policies for long-term air pollution control in the local or regional scale.

The effects of emission control on air pollutants during this G20 Summit have been investigated by several studies using field observations and numerical models. It is demonstrated that almost all major air pollutants including SO_2, NO_x (Li et al. 2019; Wu et al. 2019), fine particles (Ji et al. 2018; Li et al. 2019; Yu et al. 2018; Wu et al. 2019), and VOCs (Zheng et al. 2019) have been significantly reduced during the 14-day control period, except O3. Su et al. (2017) monitored the vertical profiles of ozone concentration in the lower troposphere of Hangzhou during the control period by using an ozone lidar. It was found that the ozone concentrations peaked near the top of the planetary boundary layer, and the temporary measures took no immediate effect on ozone pollution. Wu et al. (2019) investigated the variation of air pollution in Hangzhou and its surrounding areas during the G20

summit by using monitoring data from five sites, and reported that the air quality had been greatly improved by the implementation of the emission control. However, the average O_3 concentration was increased by 19% compared to the same periods of the five preceding years. This unique response of ozone pollution to control measures is not well understood, and of great research interest for better control of ozone pollution in the future.

To this end, a regional air quality model, within the framework of the Model Inter-Comparison Study for ASIA phase III (Li et al., 2019), is used to investigate the spatial-temporal characteristics of ozone pollution in Hangzhou during the G20 Summit in the present work. Process analysis is conducted to understand the chemical and physical factors that contribute to O_3 abundance. It is found that the serious ozone pollution happened, mainly resultant from the local photochemical reactions which are not under good control by the emission reduction measures."

2. There was no analysis of whether or not the observations at 96 sites violated the ozone standard during the G20 meeting?

Reply: Following the reviewer's suggestion, the observations at 96 sites are analyzed. Fig. 3c shows that during the 14-day emission control period of G20 summit, 52% of the observed ozone samples from the 96 sites are above the China's national level-II standard (160μg/m^3). This result confirms that regional ozone pollution appears in the YRD region during the study period. Relevant statement has been added into the revised manuscript (Line 309-312), and attached as below.

"This phenomenon is consistent with the satellite-derived tropospheric O_3 distribution in the area (Su et al. 2017), and is also supported by the observed ozone data from the 96 sites in the YRD region as shown in Fig. 3c. During the 14-day emission control period of G20 summit, 52% of the observed ozone samples from the 96 sites are above the China's national level-II standard (160μg/m^3), suggesting that regional ozone pollution appears in the YRD region during the study period."

3. The choice of Hangzhou as the analysis site is also not clear. Authors say that they selected the site based on evaluation but no evaluation metric was presented to justify their decision to focus on Hangzhou. Why not use all the observations from 96 sites in your analysis to get a regional picture?

Reply: We have added two paragraphs (lines 84-122 see reply to the first comment) in the introduction to indicate why Hangzhou is chosen as the focus. Basically, the main objective of the present study is to understand the unique response of ozone increase to emission control measures while other pollutants had been significantly reduced (Li et al. 2019; Wu et al. 2019; Ji et al. 2018; Zheng et al. 2019) during the 2016 G20 Summit which was held in Hangzhou. Observations from 96 sites are also analyzed to give a regional picture (Fig. 3c), together with the model results, as attached below.

"This phenomenon is consistent with the satellite-derived tropospheric O_3 distribution in the area (Su et al. 2017), and is also supported by the observed ozone data from the 96 sites in the YRD region as shown in Fig. 3c. During the 14-day emission control period of G20 summit, 52% of the observed ozone samples from the 96 sites are above the China's national level-II standard (160μg/m^3), suggesting that regional ozone pollution appears in the YRD region during the study period."

In addition to these major concerns, below are some other specific concerns that the authors might find useful in their revision.

1) Section 2:3: Can you be a little more specific about the IPR here? Did you save the tendency terms before and after the call to each process is made in the code? For example, did you save ozone concentrations before and after the call the chemistry solver and used the difference in the process analysis?

Reply: Yes, you are right. The IPR analysis is integrated into the WRF-Chem model and all the tendency terms are saved before and after the call to each process. The difference is then used for quantitative analysis of each process. For more details, please refer to the study of Jfffries and Tonnesen (Atmospheric Environment, 1994, 28(18): 2991-3003) and the user guide of WRF-Chem.

Following the reviewer's suggestion, we have added relevant description on the IPR analysis in lines 174-183. The description is also attached as below.

"To understand the underlying mechanism of O_3 formation, individual physical and chemical processes of O_3 formation are investigated by using the integrated process rate (IPR) analysis in the WRF-Chem model (Jfffries and Tonnesen, 1994). The IPR analysis differentiates changes in pollutant concentrations from individual atmospheric process which quantitatively elucidates the contributions of each process, mainly including advection, diffusion, emission, deposition, clouds process, aerosol and gaseous chemistry. The IPR analysis has been widely applied and demonstrated to be an effective tool for investigating the relative importance of individual processes and interpreting O_3 concentrations (Goncalves et al., 2009; Tang et al., 2017; Shu et al., 2016). In the present work, we consider gas chemistry, vertical diffusion, horizontal and vertical advections as the main atmospheric processes for O_3 formation. Other processes, such as cloud process and horizontal diffusion, play minor roles and are thus not considered."

2) Table S1: For some reason, the equations did not appear correctly in the Table. Please correct.

Reply: Revised as suggested.

3) Section 2.4: Are the observations from air quality monitoring network quality controlled or did you apply any quality control procedure to the measurements before using those for evaluation?

Reply: The quality of all the observations from air quality monitoring network has been controlled by the data provider.

4) Line 255: Change "supply raw material" to "transport ozone precursors"

Reply: Revised as suggested.

5) Figure 8 shows that horizontal advection contributes much larger to the ozone increase on most

of the days but in the abstract the authors say "vertical diffusion and chemical production" are the main drivers. I did not understand how the authors concluded this in the abstract.

Reply: Sorry for the confusion. Although horizontal advection contributes much larger to the ozone increase on most of the days, the contribution of vertical advection is also larger. The effects of these two processes have been cancelled out during several circulations. As a result, photochemical production and vertical diffusion from the upper-air background ozone are the main drivers for the local ozone. To be clear, we have modified the relevant statements in the abstract and conclusions, as attached below.

"Interesting horizontal and vertical advection circulations of O_3 are observed during several short periods, and the effects of these processes are nearly cancelled out. As a result, the ozone pollution is mainly attributed to the local photochemical reactions which are not obviously influenced by the emission reduction measures. The ratio of reduction of Volatile Organic Compounds (VOCs) to that of NO_x is a critical parameter that needs to be carefully considered for future alleviation of ozone formation. In addition, the vertical diffusion from the upper-air background O_3 also plays an important role in shaping the surface ozone concentration."

"Horizontal and vertical advection circulations are captured in Hangzhou, with horizontal advection the source and vertical advection the sink of the surface O_3 in Hangzhou. Consequently, the serious ozone pollution is mainly resultant from the local photochemical reactions which are not under good control by the emission reduction measures. As the surface O_3 formation in Hangzhou is dominant by the VOCs-limited regime, the significant reduction of NO_x compared to that of VOCs is unfavorable to chemical generation of O_3. The ratio of reduction of VOCs to that of NO_x based on the O_3-NO_x-VOCs sensitivity analysis is a critical parameter for reduction of ozone formation from photochemical reactions. In addition, it is found that the vertical diffusion from the upper-air notable background O_3 also plays an important role in shaping the surface ozone concentration when the photochemical reactions are weak. "

Referee #2

1. The authors mentioned emergency emission control measures. Were emissions perturbated to represent these measures? How did emission control measures contribute to the ozone episode?

Reply: Yes, emissions are perturbated to represent these measures. We have added two paragraphs (please refer to the reply to the first comment of Referee #1) to introduce the background of emergency emission control measures and the effects on pollutant emissions during the G20 summit. Previous studies have demonstrated that almost all major air pollutants including SO_2, NO_x (Li et al. 2019; Wu et al. 2019), fine particles (Ji et al. 2018; Li et al. 2019; Yu et al. 2018; Wu et al. 2019), and VOCs (Zheng et al. 2019) have been significantly reduced during the 14-day control period, except O_3. It was found that the temporary measures took no immediate effect on ozone pollution (Su et al. 2017), or even the average O_3 concentration was increased by 19% compared to the same periods of the five preceding years (Wu et al. 2019). This unique response of ozone pollution to control measures is not well understood, and of great research interest for better control of ozone pollution in the future, which motives the present work. To obtain the quantitative effect of emission control measures on the ozone episode, scenario simulations and sensitivity analysis are required, which is beyond the scope of the current work. However, the modification of the emission inventory to reflect the control measures has been emphasized in the revised manuscript (line 169-171), as attached below.

"However, it is worth noting that these base inventories have been modified in the simulation to reflect the realistic emissions according to the control measures taken in the period presented in the introduction."

2. The authors claimed that this study revealed notable background O_3 concentrations, but it is very confusing how this conclusion was drawn. How much does it contribute to O_3 levels in the YRD?

Reply: Thank you for pointing out this issue. The background O_3 means the O_3 that vertically distributes within the planetary boundary layer. High ozone concentrations, temporarily during most day time of the emission control period and spatially from the surface to the top of the planetary

boundary layer, are observed in Hangzhou and even the whole YRD region. This can be seen from Figs. 5, 7, and 8 in the revised manuscript. The background O_3 essentially influences the surface O_3 concentration through vertical diffusion. Its quantitative contribution to the surface O_3 level in Hangzhou is different from day to day, as demonstrated in Figs 8 and 9.

3. It is not convincing that current categorization of process analysis can provide any useful information. Concluding photochemistry dominated O_3 generation does not provide any indications for O_3 pollution control. Which precursor or process are important? More in-depth analyses are needed.

***Reply*:** The IPR analysis differentiates changes in pollutant concentrations from individual atmospheric process which quantitatively elucidates the contributions of each process, mainly including advection, diffusion, emission, deposition, clouds process, aerosol and gaseous chemistry. It has been widely applied and demonstrated to be an effective tool for investigating the relative importance of individual processes and interpreting O_3 concentrations (Goncalves et al., 2009; Tang et al., 2017; Shu et al., 2016). In the present work, to understand the underlying mechanism of O_3 formation, individual physical and chemical processes of O_3 formation are investigated by using the IPR. The gas chemistry, vertical diffusion, horizontal and vertical advections are considered as the main atmospheric processes for O_3 formation. Other processes, such as cloud process and horizontal diffusion, play minor roles and are thus not considered.

Through the IPR analysis, interesting horizontal and vertical advection circulations of O_3 are observed during several short periods, and the effects of these processes are nearly cancelled out. As a result, the ozone pollution is mainly attributed to the local photochemical reactions which are not obviously influenced by the emission reduction measures. In addition, the vertical diffusion from the upper-air background O_3 also plays an important role in shaping the surface ozone concentration.

Following the reviewer's suggestion, the discussion section has been rewritten and some more in-depth discussions on the precursors of ozone formation have been added into the revised manuscript, as attached below.

"Chemical generation of O_3 is the net effect of photochemical generation and titration consumption. VOC oxidation (Jenkin et al., 1997; Sillman, 1999) in photochemical reactions provides critical oxidants (i.e., RO_2) that efficiently convert NO to NO_2, resulting in further accumulation of O_3 (Wang et al., 2017). The chemical generation of O3 is controlled by NO_x and VOCs depending on which substance is lack in the reactions. As a consequence, there are two sensitivity regimes of O_3 production, namely, the NO_x-limited and VOC-limited regimes. Previous studies have shown that the sensitivity pattern of surface O_3 formation in Hangzhou is dominant by the VOCs-limited regime (Yan *et al.* 2016; Li *et al.*, 2017; Su *et al.*, 2017). In this regime, if the regional reduction of VOCs is much higher than that of NO_x, the O_3 concentration can be reduced, otherwise if the regional reduction of VOCs is much less than that of NO_x, the inhibitory effect of NO_x on O_3 generation will be weakened, and the O_3 concentration will increase remarkably (Wang et al. 2015). According to the studies of Su et al. (2017), Zheng et al. (2019), and Wu et al. (2019), it can be deduced that NO_x has been significantly reduced by about 60%, at least two times of the reduction of VOCs in Hangzhou. The influence of stringent emission control measures on VOCs is not as immediate and effect as that on NO_x, which is associated with the fact that there was a large amount of biogenic VOC emission in Hangzhou and surrounding regions (Liu et al. 2018; Wu et al. 2020). In fact, the average temperature during the study period is as high as around 31°C (Fig. 4c), which facilitates the biogenic VOC emissions and photochemical reactions. As a result, the photochemical generation of O_3 was not under control and high concentration of ozone appeared. However, it is worth noting that after the emergent VOCs control measures had been implemented in the area during the third stage, the net generation rate of O_3 gradually reduces since September 2, 2016, leading to a period of relatively low ozone concentration together with other meteorological effects. These discussions implicate that to alleviate ozone pollution, the ratio of reduction of VOCs to that of NO_x is the key parameter based on the O_3-

NO_x-VOCs sensitivity analysis. As the biogenic VOCs are important sources of the total VOCs in the YRD region, it is necessary to balance the reduction of NO_x to make the ratio within effective regime in the future."

Minor comments:

1) Fig. 1a does not show domain 1.

***Reply*:** Domain 1 has been marked in Fig. 1a.

2) Line 119: it is confusing if assimilation of meteorological variables were used or not, how

***Reply*:** Assimilation of meteorological variables are not used in this study. To avoid confusion, "assimilated" has been corrected as "mapped" in Line 145.

3) Line 143: In June, July, and August, biomass burning emissions are important in east China, why do you ignore it?

***Reply*:** Biomass burning emissions have already been included in the emission inventory we used (2016 Multiresolution Emission Inventory for China (MEIC, 0.25° × 0.25°; http://www.meicmodel.org/)). Thus, their effect has been considered.

~~Elucidating the ozone pollution~~Spatial-temporal Variations and Process Analysis of O_3 Pollution in ~~Yangtze River Delta region~~Hangzhou during the ~~2016~~ G20 ~~summit for MICS-Asia III~~Summit

By

Zhi-zhen Ni[1], Kun Luo[1*], Yang Gao[2], Xiang Gao[1], Fei Jiang[3], Cheng Huang[4], Jian-ren Fan[1], Joshua S. Fu[5], Chang-hong Chen[4]

[1]State Key Laboratory of Clean Energy, Department of Energy Engineering, Zhejiang University, Hangzhou 310027, China

[2] Key Laboratory of Marine Environment and Ecology, Ministry of Education of China, Ocean University of China, Qingdao 266100, China

[3]International Institute for Earth System Science, Nanjing University, Nanjing, China

[4]Shanghai Academy of Environmental Sciences, Shanghai 200233, China

[5]Civil & Environmental Engineering, the University of Tennessee, Neyland, UK

Submitted to

Atmospheric Chemistry and Physics

[*]Correspondence to: ~~zjulk@zju.edu.cn~~zjulk@zju.edu.cn

Formatted: Font: 20 pt, Font color: Auto

Formatted: Font: 20 pt, Font color: Auto

Formatted: Font: 20 pt, Font color: Auto

Formatted: Font: 20 pt, Font color: Auto

Formatted: Font: (Asian) Batang, Font color: Auto

Formatted: Snap to grid

Formatted: Font: (Asian) Batang, 14 pt, Font color: Auto

Formatted: Font: (Asian) Batang, 12 pt, Font color: Auto

Formatted: Font: (Default) Times New Roman, (Asian) Batang, 12 pt, Font color: Auto

Formatted: Font: (Asian) Batang, 12 pt, Font color: Auto

Formatted: Font color: Auto

Formatted: Space Before: 0 pt, After: 0 pt

Formatted: Font: (Asian) 等线, Font color: Auto

Formatted: Line spacing: 1.5 lines

Formatted: Font: (Asian) 等线, Font color: Auto

Formatted: Justified, Line spacing: 1.5 lines

Formatted: Font: (Asian) 等线, Font color: Auto

Abstract

~~To elucidate the factors governing~~Serious urban ozone (O_3) pollution was observed during the campaign of 2016 G20 summit in ~~2016~~ Hangzhou, China, while other pollutants had been significantly reduced by the short-term emission control measures. To understand the underlying mechanism, the Weather Research Forecast with Chemistry (WRF-Chem) model ~~was~~is used to ~~simulate~~investigate the spatial and temporal O_3 ~~evolution in the Yangtze River Delta (YRD) region~~variations in Hangzhou from ~~24~~ August 24 to ~~06~~ September ~~2016.~~ 6, 2016. The model is first successfully evaluated and validated for local and regional meteorological and chemical parameters by using the ground and upper-air level observed data. High ozone concentrations, temporarily during most day time of the emission control period and spatially from the surface to the top of the planetary boundary layer, are captured in Hangzhou and even the whole YRD region. Various atmospheric processes ~~were~~are further analyzed to determine the influential factors of local ozone formation through the integrated process rate method. ~~The results indicated~~Interesting horizontal and vertical advection circulations of O_3 are observed during several short periods, and the effects of these processes are nearly cancelled out. As a result, the ozone pollution is mainly attributed to the local photochemical reactions which are not obviously influenced by the emission reduction measures. The ratio of reduction of Volatile Organic Compounds (VOCs) to that ~~both~~of NO_x is a critical parameter that needs to be carefully considered for future alleviation of ozone formation. In addition, the vertical diffusion ~~and~~from the ~~enhanced process of local chemical generation accounted for~~upper-air background O_3 also plays an important role in shaping the ~~increase of~~ surface ~~O_3~~ozone concentration ~~in Hangzhou. Local chemical generation was found to positively correlated with O_3 concentrations, with correlation coefficient of 0.77. In accordance with the tropical weather cycle, subsidence air and stagnant weather were induced. Dynamic circulations of O_3 through advection were associated with the urban heat island effect. All these factors intensified ozone pollution in Hangzhou, particularly on 25 August 2016 (O_3-8h: 98 ppb). These findings~~. These results provide insight into urban O_3

Formatted: Font: (Asian) 等线, 18 pt, Font color: Auto
Formatted: Font: (Asian) 等线, Font color: Auto
Formatted: Font: (Asian) 等线
Formatted: Font: (Asian) 等线, Font color: Auto
Formatted: Font: (Asian) 等线
Formatted: Font: (Asian) 等线
Formatted: Font: (Asian) 等线
Formatted: Font: (Asian) 等线
Formatted: Font: (Asian) 等线
Formatted: Font: (Asian) 等线, Font color: Auto
Formatted: Font: (Asian) 等线, Font color: Auto
Formatted: Font: (Asian) 等线
Formatted: Font: (Asian) 等线
Formatted: Font: (Asian) 等线
Formatted: Font: (Asian) 等线
Formatted: Font: (Asian) 等线
Formatted: Font: (Asian) 等线
Formatted: Font: (Asian) PMingLiU
Formatted: Font: (Asian) PMingLiU
Formatted: Font: (Asian) PMingLiU
Formatted: Font: (Asian) PMingLiU
Formatted: Font: (Asian) PMingLiU
Formatted: Font: (Asian) 等线
Formatted: Font: (Asian) 等线, Font color: Auto

formation ~~and dispersion during tropical cyclone events,~~in Hangzhou and support the Model Intercomparison Study Asia Phase III (MICS-Asia Phase III).

Keywords: Ozone~~, Tropical cyclone~~ pollution, WRF-Chem, Spatial-temporal variation, Process analysis, Air quality.

Formatted: Font: (Asian) 等线

Formatted: Font: (Asian) 等线, 10 pt, Font color: Auto

Formatted: Font: (Asian) 等线, Font color: Auto

Formatted: Font: (Asian) 等线

Formatted: Font: (Asian) 等线

Formatted: Font: (Asian) Times New Roman, Font color: Auto

Formatted: Font: (Asian) 等线, Font color: Auto

Formatted: Justified, Line spacing: single

Formatted: Font: (Asian) 等线, Font color: Auto

1. Introduction

Tropospheric ozone (O_3) is generated by a series of photochemical reactions involving volatile organic compounds (VOCs), nitrogen oxide (NO_x), and carbon monoxide (CO) (Wang et al., 2006). As a primary component of photochemical smog, ground-level O_3 pollution ~~exhibits~~imposes detrimental effects on human health (Ha et al., 2014; Kheirbek et al., 2013) and the ecosystem (Landry et al., 2013; Teixeira et al., 2011). ~~The contribution of outdoor air pollution sources to premature mortality may increase globally in the coming decades (Lelieveld et al., 2015).~~However, O_3 pollution is a challenging problem worldwide. O_3 levels in cities in the United States and Europe are increasing more than those in the rural areas of these regions, where peak values gradually decreased during 1990–2010 (Paoletti et al., 2014). Nagashima et al., (2017) reported that long-term (1980–2005) trends of increase in surface O_3 over Japan may be primarily attributed to the continental transport that have contributed to photochemical O_3 production. Urban O_3 pollution events ~~can~~have also be observed in developing countries, such as Thailand (Zhang and Kim Oanh, 2002) and India (Calfapietra et al., 2016).

~~Air quality has been deteriorating in China as urbanization and motorization have progressed.~~ Many field monitoring and modeling studies have investigated the photochemical characteristics of near-surface O_3 pollution (Tang et al., 2009, 2012; Wang et al., 2013, 2014), the photochemistry of O_3 and its precursors (Xie et al., 2014), the interactions ~~of~~between O_3 ~~with~~and $PM_{2.5}$ (Shi et al., 2015), and the urban O_3 formation (Tie et al., 2013). ~~In~~It is clear that in addition to anthropogenic emissions of O_3 precursors, uncontrollable physical and chemical processes involved in meteorological phenomena ~~critically~~significantly modulate changes in O_3 concentration (Xue et al., 2014). In the Yangtze River Delta (YRD) region of China, high O_3 concentrations ~~are associated with pollutant transport and diffusion from surrounding areas~~have been observed (Gao et al., 2016; Jiang et al., 2012). Synoptic patterns related to tropical cyclones may be ~~conducive to~~one reason for such high O_3 concentrations (Huang et al., 2005). Jiang et al. (2015) reported that enhanced stratosphere–troposphere exchange (STE) driven by a tropical cyclone abruptly increased O_3 concentrations (21–

Formatted ... [64]
Formatted ... [65]
Formatted ... [66]
Formatted ... [67]
Formatted ... [68]
Formatted ... [69]
Formatted ... [70]
Formatted ... [71]
Formatted ... [72]
Formatted ... [73]
Formatted ... [74]
Formatted ... [75]
Formatted ... [76]
Formatted ... [77]
Formatted ... [78]
Formatted ... [79]
Formatted ... [80]
Formatted ... [81]
Formatted ... [82]
Formatted ... [83]
Formatted ... [84]
Formatted ... [85]
Formatted ... [86]
Formatted ... [87]
Formatted ... [88]
Formatted ... [89]
Formatted ... [90]
Formatted ... [91]
Formatted ... [92]
Formatted ... [93]
Formatted ... [94]
Formatted ... [95]
Formatted ... [96]
Formatted ... [97]
Formatted ... [98]
Formatted ... [99]
Formatted ... [100]
Formatted ... [101]
Formatted ... [102]
Formatted ... [103]
Formatted ... [104]
Formatted ... [105]
Formatted ... [106]
Formatted ... [107]
Formatted ... [108]
Formatted ... [109]
Formatted ... [110]
Formatted ... [111]

42 ppb) in the southeast of China during June 12–14, 2014~~. STE~~, which has been highlighted as ~~a significant~~another contributor to near-surface O_3 concentrations under certain conditions (Lin et al., 2012, 2015). ~~Because relevant data are limited~~However, the complex dynamics in atmospheric processes related to O_3 formation are so difficult to ~~evaluate, and the main processes that account for high O_3 concentrations are challenging to~~ identify~~.~~ that the O_3 pollution characteristics and underlying causes have not ~~been sufficiently investigated in China, especially in relation to extreme meteorological conditions. The lack of relevant data may influence urban pollution prevention efforts~~yet been well understood.

Hangzhou, the capital of Zhejiang Province, is located in the center of the Yangtze River Delta which is one of the most developed areas in China. Resultant from local emissions (Wu et al. 2014, Hu et al. 2015) and transboundary transport of aerosol and trace gases transport (Liu et al. 2015; Ni et al. 2018; Zhang et al. 2018), air pollution in Hangzhou has become serious in the recent years. In 2016, Hangzhou city would host the 2016 G20 (Group of Twenty Finance Ministers and Central Bank Governors) summit during September 4-6. To improve air quality for this event, 14-day temporarily strict air pollution alleviation measures had been taken to reduce air pollutant emissions in Hangzhou and surrounding areas from August 24 to September 6, 2016. The emission control scheme includes a coal-fired power plant capacity 50% reduction since August 24, followed by an "odd-even" on-road vehicle restriction since August 28, and further emergent VOC reduction from industrial sectors since September 1 to 6 (Ji et al. 2018; Li et al. 2019; Wu et al. 2019). ~~In this study~~These short-term measures provide a valuable opportunity to investigate the response of air quality to the emission reduction, understand the formation mechanisms of air pollution, and explore effective policies for long-term air pollution control in the local or regional scale.

The effects of emission control on air pollutants during this G20 Summit have been investigated by several studies using field observations and numerical models. It is demonstrated that almost all major air pollutants including SO_2, NO_x (Li et al. 2019; Wu et al. 2019), fine particles (Ji et al. 2018; Li et al. 2019; Yu et al. 2018; Wu et al. 2019), and VOCs (Zheng et al. 2019) have been significantly

Formatted: Font: (Asian) 等线, Font color: Auto
Formatted: Font: (Asian) 等线, Font color: Auto
Formatted: Font: (Asian) 等线
Formatted: Font: (Asian) 等线, Font color: Auto
Formatted: Font: (Asian) 等线, Font color: Auto
Formatted: Font: (Asian) 等线, Font color: Auto
Formatted: Font: (Asian) 等线
Formatted: Font: (Asian) 等线, Font color: Auto
Formatted: Font: (Asian) 等线, Font color: Auto
Formatted: Font: (Asian) 等线, Font color: Auto
Formatted: Font: (Asian) 等线, Font color: Auto
Formatted: Font: (Asian) 等线
Formatted: Font: (Asian) 等线, Font color: Auto
Formatted: Font: (Asian) 等线, Font color: Auto
Formatted: Font: (Asian) 等线, Font color: Auto

reduced during the 14-day control period, except O3. Su et al. (2017) monitored the vertical profiles of ozone concentration in the lower troposphere of Hangzhou during the control period by using an ozone lidar. It was found that the ozone concentrations peaked near the top of the planetary boundary layer, and the temporary measures took no immediate effect on ozone pollution. Wu et al. (2019) investigated the variation of air pollution in Hangzhou and its surrounding areas during the G20 summit by using monitoring data from five sites, and reported that the air quality had been greatly improved by the implementation of the emission control. However, the average O_3 concentration was increased by 19% compared to the same periods of the five preceding years. This unique response of ozone pollution to control measures is not well understood, and of great research interest for better control of ozone pollution in the future.

To this end, a regional air quality model, within the framework of the Model Inter-Comparison Study for ASIA phase III (~~MICS-ASIA-III)~~ (Li et al., 2019), ~~was~~is used to ~~elucidate~~investigate the spatial-temporal characteristics of ozone pollution in Hangzhou during the G20 Summit in the present work. Process analysis is conducted to understand the chemical and physical factors that ~~contributed~~contribute to O_3 abundance ~~during the G20 (Group of Twenty) summit. The summit was held in Hangzhou, China, and the focus of the summit was~~. It is found that the ~~sustainable and healthy development of~~ serious ozone pollution happened, mainly resultant from the ~~world economy. Emergency~~ local photochemical reactions which are not under good control by the emission ~~control~~reduction measures ~~(e.g., industrial stoppages, limitations of vehicle movement) were implemented over an area with a diameter of approximately 600 km to improve the air quality from 24 August to 06 September 2016. Because of severe concerns regarding O_3 concentrations and the summer cyclonic weather pattern, the aforementioned pollution control event attracted wide policy-related interest~~. The rest of this paper is organized as follows. Section 2 outlines the methodology and configuration of the model system. Section 3 ~~describes~~presents the ~~synoptic weather conditions as well as individual O_3 formation~~ model evaluation, the spatial-temporal characteristics of ozone

Formatted: Font: (Asian) 等线, Font color: Auto
Formatted: Indent: First line: 0.85 cm
Formatted: Font: (Asian) 等线, Font color: Auto
Formatted: Font: (Asian) 等线, Font color: Auto
Formatted: Font: (Asian) 等线, Font color: Auto
Formatted: Font: (Asian) 等线, Font color: Auto
Formatted: Font: (Asian) 等线
Formatted: Font: (Asian) 等线, Font color: Auto
Formatted: Font: (Asian) 等线, Font color: Auto
Formatted: Font: (Asian) 等线, Font color: Auto
Formatted: Font: (Asian) 等线, Font color: Auto
Formatted: Font: (Asian) 等线, Font color: Auto
Formatted: Font: (Asian) 等线, Font color: Auto

pollution, and the analysis of related atmospheric processes. Section 4 discusses the underlying causes of O_3 pollution. Finally, ~~section 5 presents~~ a summary ~~of the findings~~is made.

2. Methodology

2.1. Regional chemistry modeling system

To investigate the interactions among emissions, meteorological phenomena, and chemical phenomena, the Weather Research Forecast with Chemistry model (WRF-Chem) ~~was~~is used ~~to simulate temporal and spatial changes~~ in ~~O_3 concentration.~~the present study. The WRF-Chem is a regional online-coupled air quality model that can simultaneously ~~simulates~~simulate air quality components and meteorological components by using identical transport schemes, grid structures, and physical schemes (Grell et al., 2005). Two model domains ~~were~~are designed ~~in this study (Fig. 1a):~~: an outer domain (horizontal resolution: 30 km) covering East China (20.0°N–44.5°N, 99.0°E–126.5°E) and an inner domain (horizontal resolution: 6 km) covering the YRD region (27.6°N–32.7°N, 116.9°E–122.4°E~~).~~), as shown in Fig.1. The “Lambert conformal conic” projection ~~was~~is applied with the domain center at 34°N, 111°E. ~~There is a~~A total of 31 vertical layers are used with the model top at 50 hPa. The simulation period ~~was~~is from 17 August to ~~06~~6 September 2016, and ~~simulations of~~ the first-~~-~~week ~~were~~simulation is used to spin up the model. Hourly model outputs for 24 August to 06 September ~~were~~are used in the analysis. ~~Additional~~The gas mechanism CBMZ (Chemical Bond Mechanism Version Z) (Zaveri and Peters, 1999) is used for model simulations. For additional details regarding the ~~configuration of the WRF-Chem model are described in our~~model parameterization schemes, please refer to a previous study (Ni et al., 2018).

Formatted: Font: (Asian) 等线, Font color: Auto
Formatted: Font: (Asian) 等线, Font color: Auto
Formatted: Font: (Asian) 等线
Formatted: Font: (Asian) 等线, Font color: Auto
Formatted: Font: (Asian) 等线, Font color: Auto
Formatted: Font: (Asian) 等线, Font color: Auto
Formatted: First line: 0 ch
Formatted: Font: (Asian) 等线, Font color: Auto
Formatted: Font: (Asian) 等线, Font color: Auto
Formatted: Font: (Asian) 等线, Font color: Auto
Formatted: Font: (Asian) 等线, Font color: Auto
Formatted: Font: (Asian) 等线, Font color: Auto
Formatted: Font: (Asian) 等线, Font color: Auto
Formatted: Font: (Asian) 等线, Font color: Auto
Formatted: Font: (Asian) 等线, Font color: Auto
Formatted: Font: (Asian) 等线, Font color: Auto
Formatted: Font: (Asian) 等线, Font color: Auto
Formatted: Font: (Asian) 等线, Font color: Auto
Formatted: Font: (Asian) 等线, Font color: Auto
Formatted: Font: (Asian) 等线, Font color: Auto
Formatted: Font: (Asian) 等线, Font color: Auto
Formatted: Font: (Asian) 等线, Font color: Auto
Formatted: Font: (Asian) 等线, Font color: Auto
Formatted: Font: (Asian) 等线, Font color: Auto
Formatted: Font: (Asian) 等线, Font color: Auto
Formatted: Font: (Asian) 等线, Font color: Auto
Formatted: Font: (Asian) 等线, Font color: Auto
Formatted: Font: (Asian) 等线, Font color: Auto

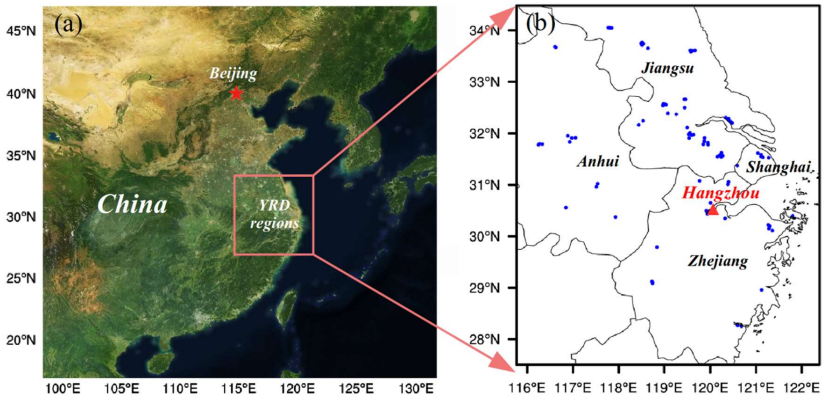

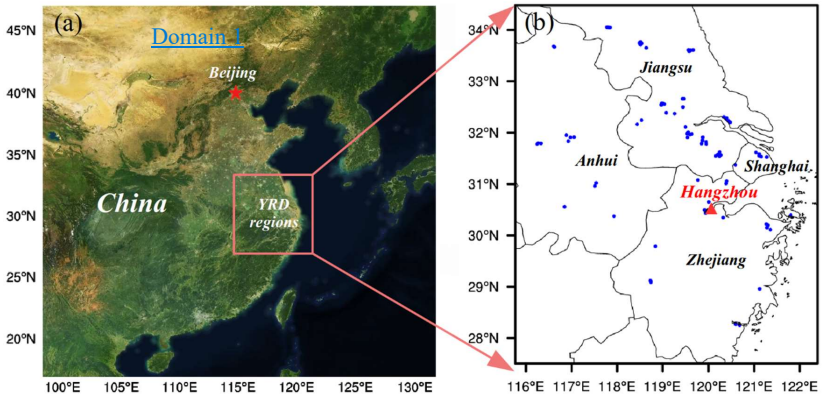

Fig. ~~1~~1. Double-nested simulation domains. (a) Domain 1: 30 km in East China with 102 (W–E) × 111 (S–N) × 31 (vertical layers) grids; (b) Domain 2: 6 km in the Yangtze River Delta (YRD) region with 100 (W–E) × 115 (S–N) × 31 (vertical layers) grids. Blue dots denote the air quality monitoring sites. The copyright of the background map belongs to Google Map © Microsoft.

The meteorological boundary and initial conditions ~~were~~are determined from the global objective final analysis (FNL) data of the National Centers for Environmental Prediction (Kalnay et al., 1996). The FNL data ~~were also assimilated~~are mapped to domain 1 (East China), and the grid-nudging method (Stauffer et al., 1991) ~~was~~is used to reduce the meteorological integral errors. The chemical initial and boundary conditions ~~were~~are dynamically downscaled from the simulation results of model for ozone and related chemical tracers, version 4 (MOZART4) (Emmons et al., 2010~~)~~

Formatted: Font: (Asian) 等线, Font color: Auto
Formatted: Font: (Asian) 等线, Font color: Auto
Formatted: Font: (Asian) 等线
Formatted: Font: (Asian) 等线, Font color: Auto
Formatted: Font: (Asian) Times New Roman, Font color: Auto
Formatted: First line: 0 ch
Formatted: Font: (Asian) 等线, Font color: Auto
Formatted: Font: (Asian) 等线, Font color: Auto
Formatted: Font: (Asian) 等线, Font color: Auto
Formatted: Font: (Asian) 等线, Font color: Auto
Formatted: Font: (Asian) 等线, Font color: Auto

~~simulation results; the relevant data are available at https://www.acom.ucar.edu/wrf-chem/mozart.shtml.~~).

2.2. Emissions

The 2016 Multiresolution Emission Inventory for China (MEIC, 0.25° × 0.25°; ~~http://www.meicmodel.org/~~http://www.meicmodel.org/) ~~was~~is used for the outer domain (Fig. 1a) with a spatial resolution of 30 km (Li et al., 2017), including species of SO_2, NO_x, CO, NH_3, PM2.5, and VOCs from the power, industrial, residential, transportation, and agricultural sectors. Inventories of finer anthropogenic emissions for the YRD region ~~(Fig. 1b)~~ over the year of 2014 ~~were~~ compiled ~~based on the bottom-up method~~ by Shanghai Academy of Environmental Sciences~~.~~ are used for the inner domain (Fig. 1b). These inventories have been well documented in ~~detail in~~ previous studies (Huang et al., 2011; Li et al., 2011; Liu et al., 2018). ~~Thus, only brief discussions of these inventories are presented herein.~~ The fine emission inventories include major sectors such as large point sources, industrial sources, mobile sources, and residential sources. The anthropogenic emissions over the YRD region are mainly located over the industrial and urban areas along the Yangtze River as well as over Hangzhou Bay. In this study, the emission inventories for the two domains ~~were~~are projected into horizontal and vertical grids as hourly emissions, with temporal and vertical profiles obtained from Wang et al. (2011). VOCs emissions ~~were~~are categorized into modeled species, according to von Schneidemesser et al. (2016). In addition, biogenic emissions ~~were~~are generated offline using the Model of Emission of Gases and Aerosols from Nature (MEGAN) (Guenther et al., 2006). Dust emissions ~~were~~are calculated online from surface features and meteorological fields by using the Air Force Weather Agency and Atmospheric and Environmental Research scheme (Jones et al., 2011). Other emissions ~~(i.e.,~~ such as those from biomass burning, aviation, and sailing ships~~),~~ accounting for very small ~~fractions~~fraction during this period, ~~were~~are therefore not considered here. However, it is worth noting that these base inventories have been modified in ~~this study~~the simulation to reflect the realistic emissions according to the control measures taken in the period presented in the introduction.

Formatted: Font: (Asian) 等线, Font color: Auto

Formatted: Default Paragraph Font, Font color: Auto

Formatted: Font color: Auto

Formatted ... [112]

2.3. Atmospheric processes analysis

To understand the ~~mechanism~~ underlying mechanism of O_3 formation, individual physical and chemical processes of O_3 formation ~~were~~are investigated by using the integrated process rate (IPR) analysis in the WRF-Chem model~~.~~ (Jfffries and Tonnesen, 1994). The IPR analysis differentiates changes in pollutant concentrations from individual atmospheric process which quantitatively elucidates the contributions of each process, mainly including advection, diffusion, emission, deposition, clouds process, aerosol and gaseous chemistry. The IPR analysis has been widely applied~~;~~ ~~this method has been proven~~ and demonstrated to be an effective tool for ~~demonstrating~~investigating the relative importance of individual processes and ~~for~~ interpreting O_3 concentrations (Goncalves et al., 2009; Tang et al., 2017; Shu et al., 2016). ~~The~~In the present ~~study investigated atmospheric processes involved in O_3 formation, including~~ work, we consider gas chemistry, vertical diffusion, ~~and~~ horizontal and vertical ~~advection.~~advections as the main atmospheric processes for O_3 formation. Other processes ~~(i.e., such as~~ cloud ~~processes~~process and horizontal diffusion~~) that either~~ play minor roles ~~or result in the formation of a sink (i.e., dry and wet deposition) were~~and are thus not considered ~~in this study.~~

2.4. Evaluation ~~method~~metrics

To increase the confidence in interpretations of model results, model outputs should first be evaluated based on observations. Accordingly, ~~in this study,~~ the model results derived from domain 2 ~~were~~are compared with hourly surface observational data obtained from 96 air quality monitoring sites in the YRD region (blue dots, Fig. ~~1b). These data were downloaded from http://www.pm25.in. The air pollutants assessed were O_3 and NO_2. Model performance was evaluated using statistical measures, namely mean fractional bias (MFB), mean fractional error (MFE), and correlation coefficient (R), following the recommendation of the US Environmental Protection Agency (US EPA; 2007). The formula used in this evaluation is presented in Table S1. Additionally, the meteorological parameters were evaluated based on observational data—including temperature at 2 m (T2), relative humidity at 2 m (RH2), and 10 m wind speed (WS10) and direction (WD10)—from the~~

Formatted: Font: (Asian) 等线, Font color: Auto
Formatted: Font: (Asian) 等线, Font color: Auto
Formatted: First line: 0 ch
Formatted: Font: (Asian) 等线
Formatted: Font: (Asian) 等线, Font color: Auto
Formatted: Font: (Asian) 等线, Font color: Auto
Formatted: Font: (Asian) 等线, Font color: Auto
Formatted: Font: (Asian) 等线, Font color: Auto
Formatted: Font: (Asian) 等线, Font color: Auto
Formatted: Font: (Asian) 等线, Font color: Auto
Formatted: Font: (Asian) 等线, Font color: Auto
Formatted: Font: (Asian) 等线
Formatted: Font: (Asian) 等线, Font color: Auto
Formatted: Font: (Asian) 等线, Font color: Auto
Formatted: Font: (Asian) 等线, Font color: Auto
Formatted: Font: (Asian) 等线, Font color: Auto
Formatted: Font: (Asian) 等线, Font color: Auto
Formatted: Font: (Asian) 等线, Font color: Auto
Formatted: Font: (Asian) 等线, Font color: Auto
Formatted: Font: (Asian) 等线, Font color: Auto
Formatted: Font: (Asian) 等线, Font color: Auto
Formatted: Font: (Asian) 等线, Font color: Auto
Formatted: Font color: Auto
Formatted: Font color: Auto
Formatted: Font color: Auto
Formatted: Font color: Auto

~~Meteorological Assimilation Data Ingest System~~ 1b) in this study. These observational data are downloaded from http://www.pm25.in, and O_3 as well as its precursor NO_2 are evaluated, in terms of statistical measures, namely the mean fractional bias (MFB), the mean fractional error (MFE), and the correlation coefficient (R), following the recommendation of the US Environmental Protection Agency (US EPA, 2007). Additionally, the meteorological parameters are evaluated based on the observational data, including temperature at 2 m (T2), relative humidity at 2 m (RH2), 10 m wind speed (WS10) and direction (WD10), from the Meteorological Assimilation Data Ingest System

Table 1. Discrete statistical indicators used in the model evaluation

Metrics	Definition	Range
Mean Fractional Bias (MFB)	$MFB = \frac{2}{N}\sum_{i=1}^{N}\frac{S_i - O_i}{S_i + O_i} \times 100\%$	-200% to 200%
Mean Fractional Error (MFE)	$MFE = \frac{2}{N}\sum_{i=1}^{N}\frac{\lvert S_i - O_i\rvert}{S_i + O_i} \times 100\%$	0 to 200%
Correlation Coefficient (r)	$r = \frac{\sum_{i=1}^{N}(S_i - \bar{S})(O_i - \bar{O})}{\sqrt{\sum_{i=1}^{N}(S_i - \bar{S})^2 \sum_{i=1}^{N}(O_i - \bar{O})^2}}$	0 to 1
Mean Bias (MB)	$MB = \frac{1}{N}\sum_{i=1}^{N}(S_i - O_i)$	-∞ to +∞
Gross Error (GE)	$GE = \frac{1}{N}\sum_{i=1}^{N}\lvert S_i - O_i\rvert$	0 to +∞
Root Mean Square Error (RMSE)	$RMSE = \sqrt{\frac{1}{N}\sum_{i=1}^{N}(S_i - O_i)^2}$	0 to +∞

N is the number of samples. S_i and O_i are values of simulations and observations at time or location i, respectively.

(https://madis.noaa.gov). Following the study of Zhang et al. (2014), commonly used mean bias (MB), gross error (GE), and root mean square error (RMSE) ~~were~~are calculated as the statistical indicators~~; corresponding equations are denoted~~. All used statistical indicators are summarized in Table ~~S1~~1.

~~The~~Besides the above evaluation of single-point based time series results, the vertical spatial distribution of modeled O_3 in Hangzhou ~~was~~is also evaluated ~~based on~~by comparisons with observed differential absorption LiDAR (DIAL) data (Su et al. 2017). In the DIAL technique, the mean gas concentration over a certain range interval is determined by analyzing the LiDAR backscatter signals

Formatted: Font color: Auto
Formatted: Normal, Justified, Indent: First line: 0 ch
Formatted: Default Paragraph Font, Font color: Auto
Formatted: Default Paragraph Font, Font color: Auto
Formatted: Default Paragraph Font, Font color: Auto
Formatted: Default Paragraph Font, Font color: Auto
Formatted: Font color: Auto
Formatted: First line: 0 ch
Formatted: Font: (Asian) 等线, Font color: Auto
Formatted: Font: (Asian) 等线, Font color: Auto
Formatted: Font: (Asian) 等线
Formatted: Font: (Asian) 等线, Font color: Auto
Formatted: Font: (Asian) 等线, Font color: Auto
Formatted: Font: (Asian) 等线, Font color: Auto

for laser wavelengths tuned "on" (λ_{on}) and "off" (λ_{off}) in a molecular absorption peak of the gas under investigation (Browell et al., 1998). The DIAL technique can be used to measure O_3 concentrations above or near a specific location (Browell, 1989). In our DIAL datasets, the vertical height available was from 0.3 km to 3 km due to the limitations of the signal-to-noise ratio and detection range.

Formatted: Font: (Asian) 等线
Formatted: Font: (Asian) 等线, Font color: Auto
Formatted: Font: (Asian) 等线
Formatted: Font: (Asian) 等线, Font color: Auto
Formatted: Font: (Asian) 等线
Formatted: Font: (Asian) 等线, Font color: Auto
Formatted: Font: (Asian) 等线, Font color: Auto

3. Results

3.1. Model performance evaluation

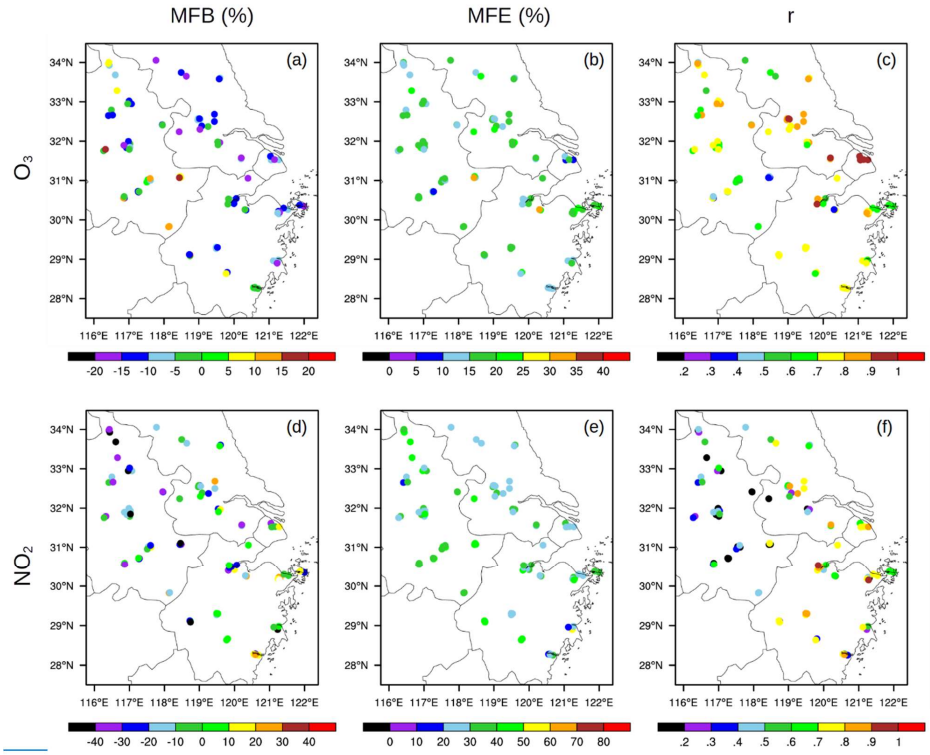

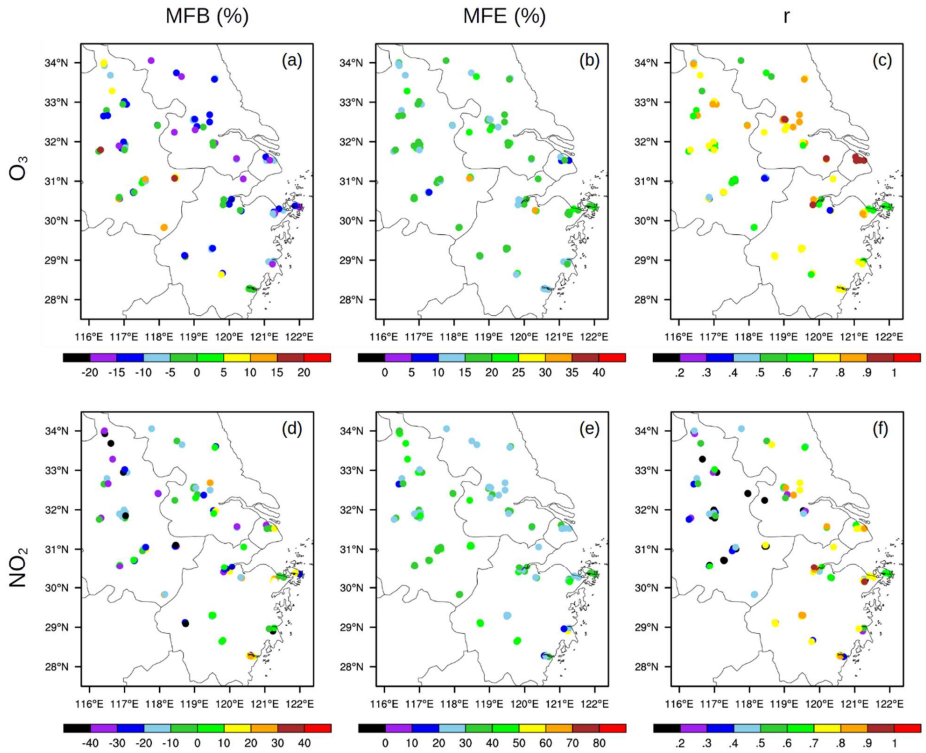

Fig. 2. Comparison of modeled air ~~pollutants~~pollutant concentrations against measurements in 96 monitoring sites over YRD region during August 24–September 6, 2016: Mean fractional bias (MFB), mean fractional error (MFE) and Pearson's correlation coefficient (r) of O_3 (a–c) and NO_2 (d–f), respectively.

investigation (Browell et al., 1998). In the DIAL data of O_3, the vertical height available is from 0.3 km to 3 km due to the limitations of the signal-to-noise ratio and detection range.

3. Results

3.1. Model performance

We first ~~evaluated~~evaluate the overall performance of WRF-Chem for the YRD region by incorporating data from the 96 air quality monitoring sites. Specifically, the maximum daily 8 h (~~O3-8h~~MDA8) ozone and daily mean NO_2 concentrations at the surface ~~were~~are used. The spatial distributions of MFB and MFE for O_3 and NO_2 are illustrated in Fig. 2. In general, the model-

Formatted: Font: (Asian) 等线, Font color: Auto
Formatted: Font: (Asian) 等线
Formatted: Font: (Asian) 等线, Font color: Auto
Formatted: Font: (Asian) 等线
Formatted: Font: (Asian) 等线, Font color: Auto
Formatted: Font: (Asian) 等线, Font color: Auto
Formatted: Font: (Asian) 等线
Formatted: Font: (Asian) 等线
Formatted: Font: (Asian) 等线, Font color: Auto
Formatted: Font: (Asian) PMingLiU
Formatted: Font: (Asian) 等线
Formatted: Font: (Asian) PMingLiU

simulated air pollutant concentrations ~~agreed~~agree well with the observations~~. The spatial distributions of MFB and MFE for O_3 and NO_2 at the 96 observational sites over the YRD region are illustrated in Fig. 2. The results reflected reasonable performance~~, with MFB and MFE for most of the sites meeting

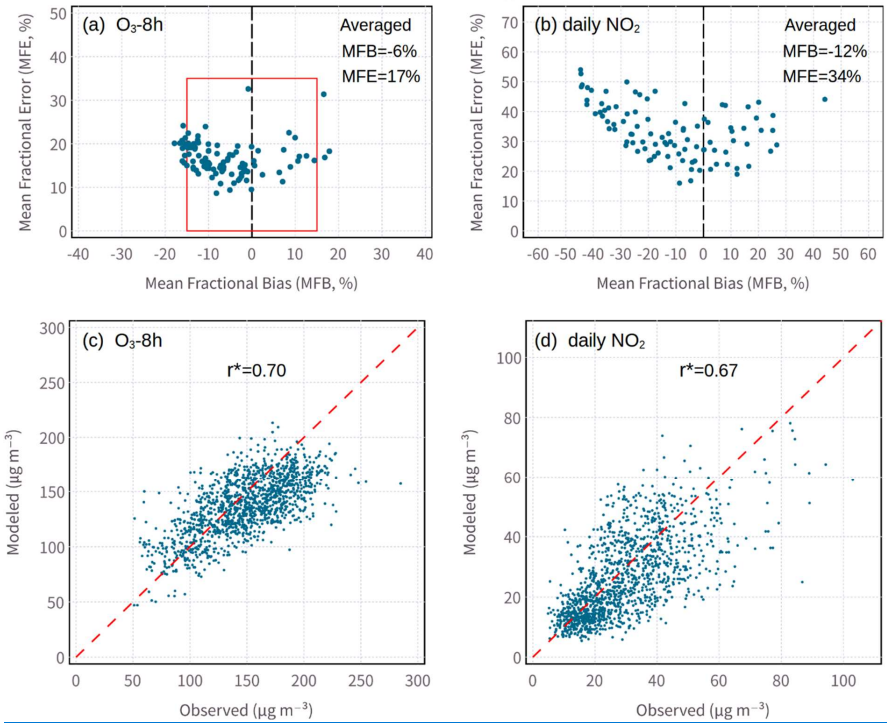

Fig. 3. Comparisons of modeled and observed concentrations of the air pollutants from 96 air quality monitoring sites across the YRD from 24 August to 06 September 2016 (1,344 pairs). Scatter plots for MFB and MFE of (a) O_3 and (b) NO_2. Performance goals (red box) for O_3 are the benchmarks. Scatter plots for daily observed and modeled (c) O_3 and (d) NO_2.

the benchmarks (MFB~~:~~ <15%; MFE~~:~~ <35%) ~~proposed by the US Environmental Protection Agency~~ (US EPA~~:~~, 2007). A scatter plot of MFB/MFE ~~was~~is shown in Fig. ~~S1a,b in the supporting information~~3, further ~~hinting~~demonstrating the ~~ability~~capability of the present model in reproducing the observations, which is also ~~reflected~~supported by the high correlation between model and ~~observations (observation (Fig. 3c, d). Fig. S1c,d in the supporting information). Other model~~

Formatted: Font: (Asian) 等线, Font color: Auto
Formatted: Font: (Asian) PMingLiU
Formatted: Font: (Asian) 等线, Font color: Auto
Formatted: Font: (Asian) 等线
Formatted: Font: (Asian) 等线
Formatted: Font: (Asian) 等线, 10.5 pt, Bold, Font color: Auto
Formatted: Font: (Asian) 等线, 10.5 pt, Font color: Auto
Formatted: Indent: First line: 0 ch, Tab stops: Not at 1 cm
Formatted: Font: (Asian) 等线, Font color: Auto
Formatted: Font: (Asian) 等线, Font color: Auto
Formatted: Font: (Asian) 等线, Font color: Auto
Formatted: Font: (Asian) 等线, Font color: Auto
Formatted: Font: (Asian) 等线, Font color: Auto
Formatted: Font: (Asian) 等线, Font color: Auto
Formatted: Font: (Asian) 等线, Font color: Auto
Formatted: Font: (Asian) 等线, Font color: Auto
Formatted: Font: (Asian) 等线, Font color: Auto
Formatted: Font: (Asian) 等线, Font color: Auto
Formatted: Font: (Asian) 等线, Font color: Auto
Formatted: Font: (Asian) 等线, 10.5 pt, Bold, Font color: Auto

evaluations with satellite retrievals during this period can been seen in our previous study (Ni et al., 2019).

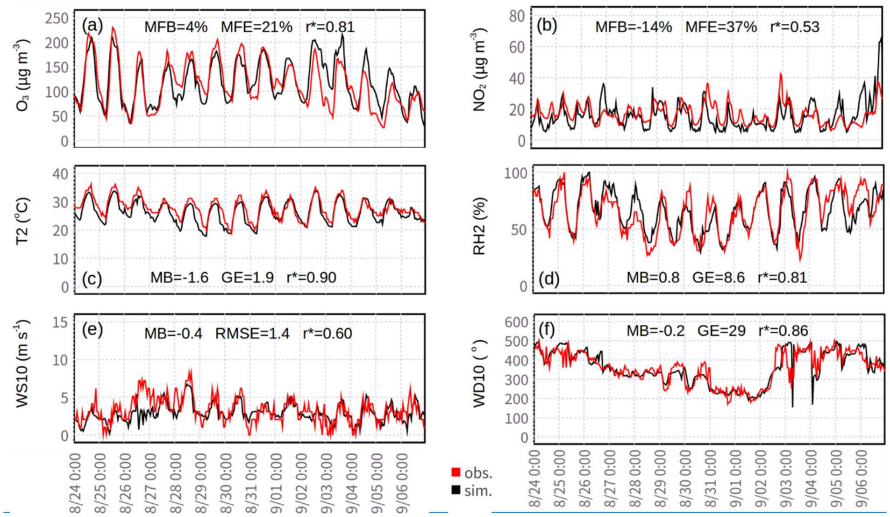

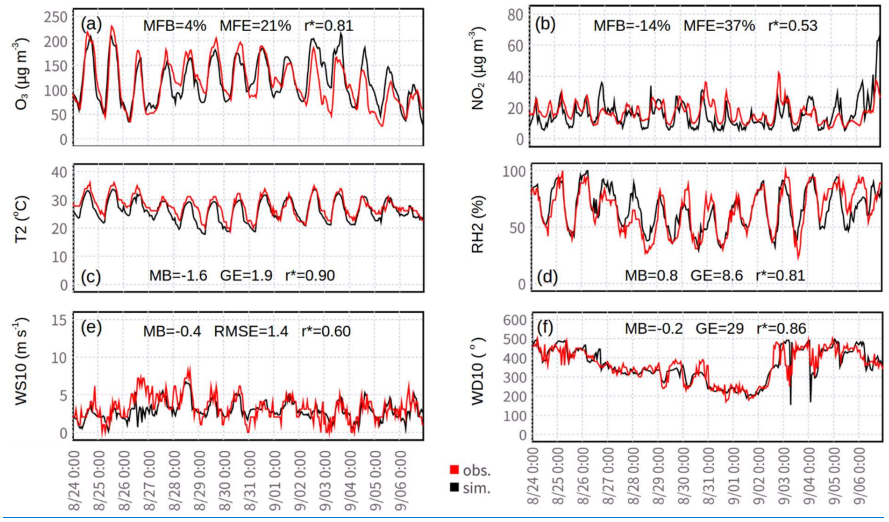

Fig. 3.4. Modeled air pollutants and meteorological parameters compared with measurements at the Hangzhou monitoring site from 24 August to 06 September 2016. Surface concentrations of (a) O_3 and (b) NO_2, (c) temperature at 2 m (T2), (d) relative humidity at 2 m (RH2), (e) wind speed at 10 m (WS10) and (f) wind direction at 10 m (WD10).

Formatted: Font: (Asian) 等线, Font color: Auto

Formatted: Font: (Asian) 等线, Font color: Auto

Formatted: Font: (Asian) 等线, Font color: Auto

Formatted: Font: (Asian) PMingLiU

Formatted: Font: (Asian) 等线, Font color: Auto

Formatted: Font: (Asian) 等线

Formatted: Font: (Asian) 等线, Font color: Auto

~~Following~~ After the above overall evaluation of the ~~greater~~present model in the whole YRD region, the site of Hangzhou ~~was~~will be focused on for further analysis~~, and WRF-Chem simulations of the site's air quality and meteorological conditions were assessed.~~. The time series of hourly simulated and observed air pollutants (O_3, Fig. ~~3a~~4a; NO_2, Fig. ~~3b~~4b) and meteorological factors (T2, Fig. ~~3c~~4c; RH2, Fig. ~~3d~~4d; WS10, Fig. ~~3e~~4e; and WD10, Fig. ~~3f)~~4f) at Hangzhou are presented in Fig. ~~3. All~~4. It is found that all modeled data ~~were~~are statistically significantly correlated with the observed data at the 95% level. ~~Overall, WRF-Chem well represented the observed diurnal variations. For example, the~~The MFB and MFE for both O_3 and NO_2 ~~were near the benchmarks in particular of O_3 levels (MFB/MFE: 4%/21%), and were~~are well below the benchmarks (MFB/MFE: 15%/35%; US EPA~~;~~, 2007~~).~~

~~For evaluation of~~) and the observed diurnal variations are well reproduced. For meteorological parameters, ~~Emery et al. (2001) proposed benchmarks, including 2 m air temperature (MB~~ ≤ ± 0.5° C, GE ≤ 2.0°C), 10 m wind speed (MB ≤ 0.5 m/s, RMSE ≤ 2.0 m/s) and 10 m wind direction (MB ≤ ± 10°, GE ≤ 30°). McNally (2009) suggested a relaxed benchmark for 2 m temperature (MB ≤ ± 1.0°C). In this study, the 10 m wind speed and wind direction (Fig. 3e, f) results ~~were~~are well within the ~~proposed limits.~~benchmarks. The GE of 2 m air temperature (1.9°C; Fig. 3c) also ~~satisfied~~satisfies the criteria~~; however,~~, but the MB ~~was~~is slightly higher (−1.6°C~~), and a slightly high temperature bias was~~) which has also been noted in a previous study (Zhang et al., 2014). ~~Overall, favorable performance was noted for~~These comparisons further demonstrate that the present model is able to correctly predict the ~~simulation~~time series of both meteorological parameters and air pollutants of O_3 and NO_2 in ~~comparison with observations~~Hangzhou.

Formatted ... [113]

Formatted: Indent: First line: 0 ch

Formatted ... [114]

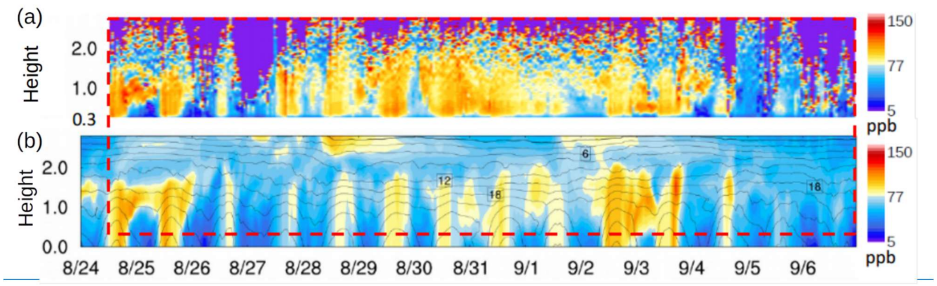

~~Fig. 4. Upper-level~~

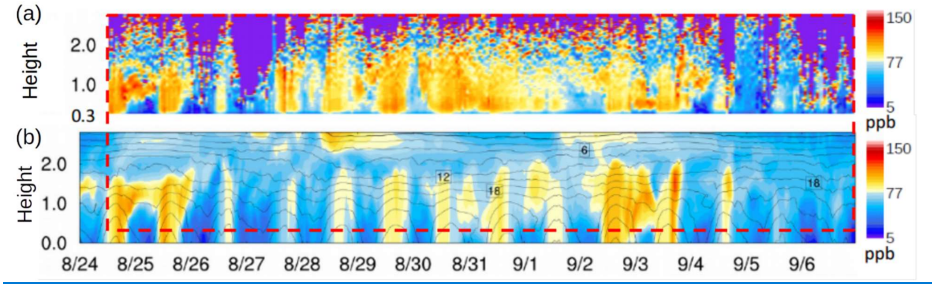

Fig. 5. Vertical comparison of hourly (a) observed (from differential absorption LiDAR) and (b) simulated O_3 concentrations (ppb) in Hangzhou ~~for~~from 24 August to 06 September 2016. Purple regions in the top panel denote invalid data with a low signal-to-noise ratio. To facilitate direct comparison, the red dashed line ~~indicates~~is added to indicate the ozone level recorded for the same time periods (starting from 12:00, 24 August) and vertical heights (0.3–3 km) in the observations and simulation results.

To further evaluate the ~~ability~~capability of the model to ~~reproduce~~predict the vertical structure of ozone concentration, the vertical distribution of the modeled O_3 ~~was~~in Hangzhou from 24 August to 06 September 2016 is qualitatively compared with the DIAL ~~datasets (~~data, as shown in Fig. 4~~).~~ ~~The comparison revealed~~5. It is interesting to find that the present model ~~results~~can successfully predict the spatial-temporal distribution of ozone in Hangzhou. All observed major features of ozone are well captured by the model. This gives us high confidence and lays a solid foundation for further exploring the pollution characteristics and influencing factors of ozone in Hangzhou during the G20 summit.

Formatted: Font: (Asian) 等线, Font color: Auto
Formatted: Font: (Asian) 等线
Formatted: Font: (Asian) 等线, Font color: Auto
Formatted: Font: (Asian) 等线
Formatted: Font: (Asian) 等线
Formatted: Font: (Asian) 等线, Font color: Auto
Formatted: Font: (Asian) PMingLiU
Formatted: Font: (Asian) 等线, Font color: Auto
Formatted: Font: (Asian) PMingLiU
Formatted: Font: (Asian) 等线, Font color: Auto
Formatted: Font: (Asian) PMingLiU
Formatted: Font: (Asian) 等线, Font color: Auto
Formatted: Font: (Asian) 等线, Font color: Auto
Formatted: Font: (Asian) 等线
Formatted: Font: (Asian) PMingLiU
Formatted: Font: (Asian) 等线, Font color: Auto

3.2. Spatial-temporal variations of O_3 pollution

To discuss spatial-temporal characteristics of O_3 pollution in Hangzhou, the whole emission control period can be divided into three stages according to the reduction intensity of the measures. August 24-27, 2016 is the first stage (S1) during which industrial and construction emission controls were implemented. During the second stage (S2, August 28-31), traffic restrictions were further added. September 1-6 2016 is the third stage (S3) with the emergent VOCs control further implemented. Figs. 4(a) and 4(b) in the above section also present the temporal evolution of O_3 and its precursor NO_2 in Hangzhou city during the emission control period of G20 summit. It is evident that the NO_2 has been significantly reduced by the emission control measures and the concentration is well below the national level-II standard of 200 μg/m^3. However, the concentration of O_3 keeps high levels for the whole 14 days, with 7 days of MDA8 are above and 4 days are close to the national level-II standard (GB-3095–2012) of 160μg/m^3. This serious O_3 pollution indicates that the emission control measures seem to make no obvious effect on ozone, which is consistent with ~~the~~previous observations~~.~~ ~~Diurnal O_3 variations were mainly observed within the planetary boundary layer (approximately <2 km). Notably, the model captured a nocturnal O_3-rich mass, which exhibited an n-shaped distribution in the upper air (approximately 1 km) on 25 August 2016.~~ (Su et al. 2017; Wu et al. 2019). The diurnal variation of O_3 is similar for the

Formatted: First line: 0 ch

Formatted: Font: (Asian) 等线, Font color: Auto

Formatted: Font: (Asian) 等线, Font color: Auto

Formatted: Font: (Asian) 等线, Font color: Auto

Formatted: Font: (Asian) 等线, Font color: Auto

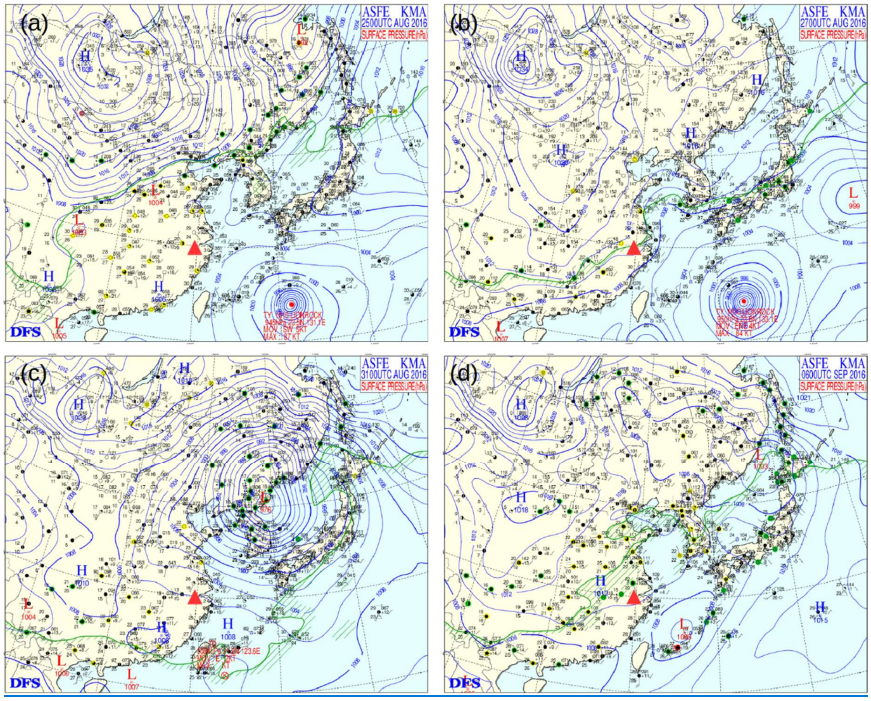
(a)
ASFE KMA
2500UTC AUG 2016
SURFACE PRESSURE(hPa)
DFS
(b)
ASFE KMA
2700UTC AUG 2016
SURFACE PRESSURE(hPa)
DFS
(c)
ASFE KMA
3100UTC AUG 2016
SURFACE PRESSURE(hPa)
DFS
(d)
ASFE KMA
0600UTC SEP 2016
SURFACE PRESSURE(hPa)
DFS

635

Fig. ~~3.2~~6. Synoptic ~~weather system~~

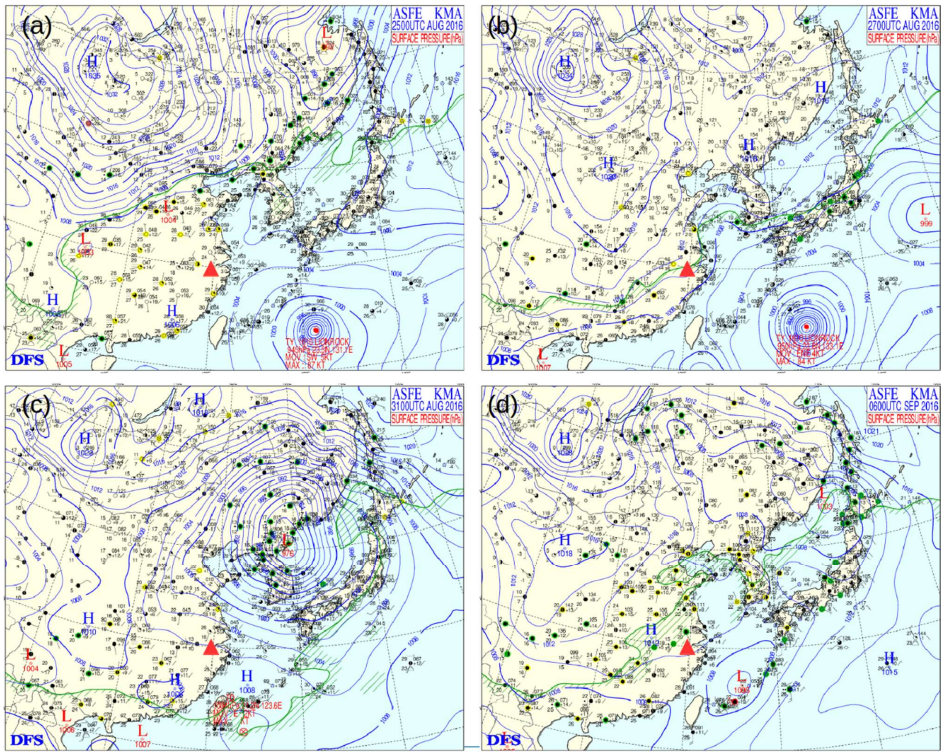

circulation. ~~**Fig. 5.** Tropical cyclone evolution~~ in East Asia during the 2016 G20 summit. Weather charts for four representative periods at 08:00 LST on (a) 25 August, (b) 27 August, (c) 31 August, and (d) 06 September 2016. LST: Local Sidereal Time; H: High-pressure system; L: Low-pressure system. The red triangle denotes the location of Hangzhou city.

three stages with a peak value at the time around 16:00 and a valley value at the time around 8:00 of each day. However, the variation magnitude in Stage 2 is obviously lower than those of other stages, which will be further discussed later.

Fig. 5 also clearly shows this diurnal variation of O_3 in the ground level. However, nocturnal O_3-rich mass is observed during certain periods in the upper air (approximately 1 km), such as August 25, August 31, and September 3, which makes an n-shaped distribution pattern of the O_3 in the upper air. This kind of spatial distribution of ozone will promote vertical exchange of O_3 in the area. In

Formatted: Font color: Auto
Formatted: Font: 10.5 pt, Font color: Auto
Formatted: Font: (Asian) 等线, Font color: Auto
Formatted: Font: (Asian) 等线, Font color: Auto
Formatted: Font: (Asian) PMingLiU
Formatted: Font: (Asian) 等线, Font color: Auto
Formatted: Font: (Asian) 等线
Formatted: Font: (Asian) 等线, Font color: Auto

general, high concentrations of O_3 appear vertically until the top of the planetary boundary layer (PBL, approximately <2 km), suggesting the ozone pollution is not a local but a regional phenomenon in the whole low-level (from surface to close to the PBL height) region.

Considering the synoptic circulation is closely related to regional O_3 abundance, four representative surface weather charts obtained from the Korea Meteorological Administration ~~were used to track the tropical cyclone~~ (are presented in Fig. ~~5).~~6. In the early stage ~~of the tropical cyclone during 24 and 25 August 2016 (Fig. 5a),~~ strong and uniform high-pressure fields covered vast regions of southeastern China~~. A~~, and a tropical cyclone moved northeastward over the East China Sea. (Fig. 6a). In the middle stage (Fig. ~~5b~~6b), the tropical cyclone approached the YRD region, bringing strong north wind fields to this area. ~~The~~As a result, the long narrow rain band arrived in Hangzhou (red triangle) on 27 August 2016. In the later stage (Fig. ~~5c~~6c), the cyclone continuously moved ~~toward Japan~~ and eventually hit the land~~. The~~, and the tropical high in the YRD region recovered gradually. Finally, the cyclone faded, and a rainstorm appeared over most of the YRD region~~. This rainstorm continued from approximately 02 through 07 September 2016 (Fig. 5d, for clarity, only the data for 06 September are presented~~ (Fig. 6d).

~~3.3. O_3 pollution episode~~

~~In Fig. 6,~~The typical hourly vertical and horizontal O_3 distributions ~~and wind fields~~ in the YRD region are further presented in Fig.7. The wind fields are also included for ~~three representative episodes according to the movement of the tropical cyclone.~~better understanding. For stagnation days with weak wind fields ~~(i.e., 25 August and 02 September)~~and strong radiation before or after the tropical cyclone, meteorological conditions ~~were~~are unfavorable for pollutant dispersion. As a result, O_3 pollution ~~was~~is more regional and intense, with an hourly peak O_3 concentration of 250 μg ~~m^{-3}~~ ~~below the high layer (2 km) around Hangzhou (Fig. 6a,c). As the cyclone approached (on 27 August), a large belt of O_3-rich mass (>160 μg m^{-3})~~/m^3 appeared ~~in the upwind direction and moved toward Hangzhou under a prevailing north wind field (Fig. 6b). Transboundary pollutant transport played a critical role~~ within the planetary boundary layer in the whole YRD region, as shown in Figs. 7a and

Formatted: Font: (Asian) 等线, Font color: Auto
Formatted: Font: (Asian) 等线, Font color: Auto
Formatted: Font: (Asian) 等线
Formatted: Font: (Asian) 等线, Font color: Auto, Not Superscript/ Subscript
Formatted: Indent: First line: 0.85 cm, Tab stops: Not at 0.99 cm
Formatted: Font: (Asian) 等线, Font color: Auto
Formatted: Font: (Asian) 等线, Font color: Auto
Formatted: Font: (Asian) 等线, Font color: Auto
Formatted: Font: (Asian) 等线, Font color: Auto
Formatted: Font: (Asian) 等线, Font color: Auto
Formatted: Font: (Asian) 等线, Font color: Auto
Formatted: Font: (Asian) 等线, Font color: Auto
Formatted: Font: (Asian) 等线, Font color: Auto
Formatted: Font: (Asian) 等线, Font color: Auto
Formatted: Font: (Asian) 等线, Font color: Auto
Formatted: Font: (Asian) 等线, Font color: Auto
Formatted: First line: 0 ch
Formatted: Font: (Asian) 等线, Font color: Auto
Formatted: Font: (Asian) 等线
Formatted: Font: (Asian) 等线, Font color: Auto
Formatted: Font: (Asian) 等线, Font color: Auto
Formatted: Font: (Asian) 等线, Font color: Auto
Formatted: Font: (Asian) 等线, Font color: Auto
Formatted: Font: (Asian) 等线, Font color: Auto
Formatted: Font: (Asian) 等线, Font color: Auto
Formatted: Font: (Asian) 等线, Font color: Auto
Formatted: Font: (Asian) 等线, Font color: Auto
Formatted: Font: (Asian) 等线
Formatted: Font: (Asian) 等线, Font color: Auto
Formatted: Font: (Asian) 等线, Font color: Auto
Formatted: Font: (Asian) 等线, Font color: Auto

7c. In these ~~processes, and this finding was consistent with the atmospheric trajectories from North China (Fig. S2). This southward transport of pollutants may supply raw materials for~~conditions, photochemical ~~O_3 generation.~~

Formatted: Font: (Asian) 等线, Font color: Auto

Formatted: Font: (Asian) 等线, Font color: Auto

Formatted: Font: (Asian) 等线, Font color: Auto

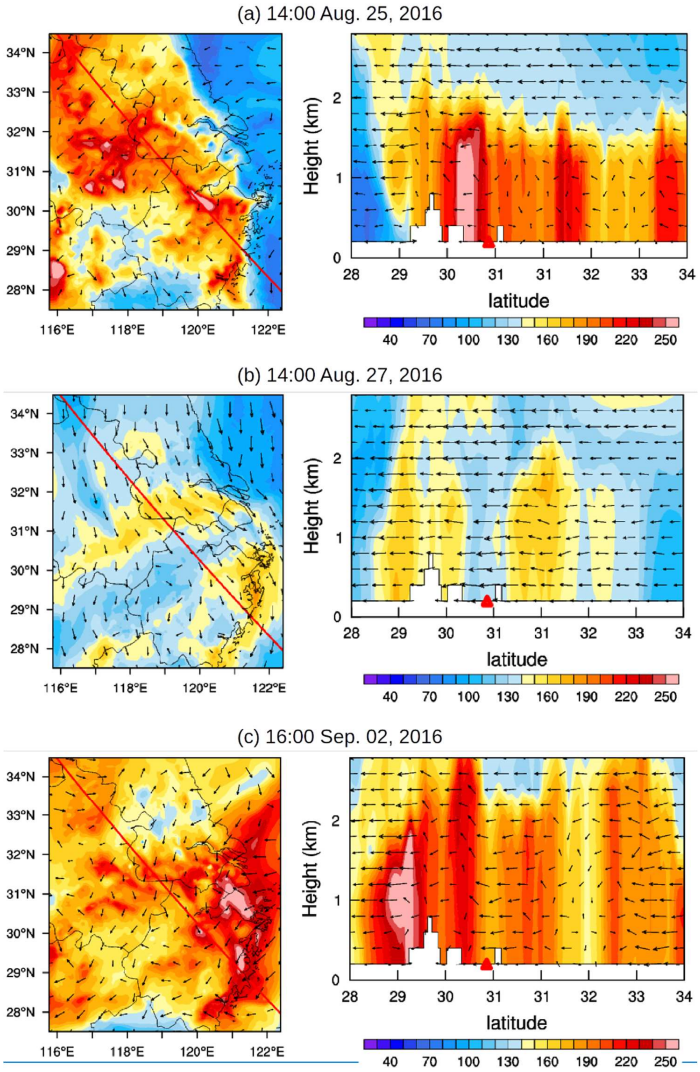

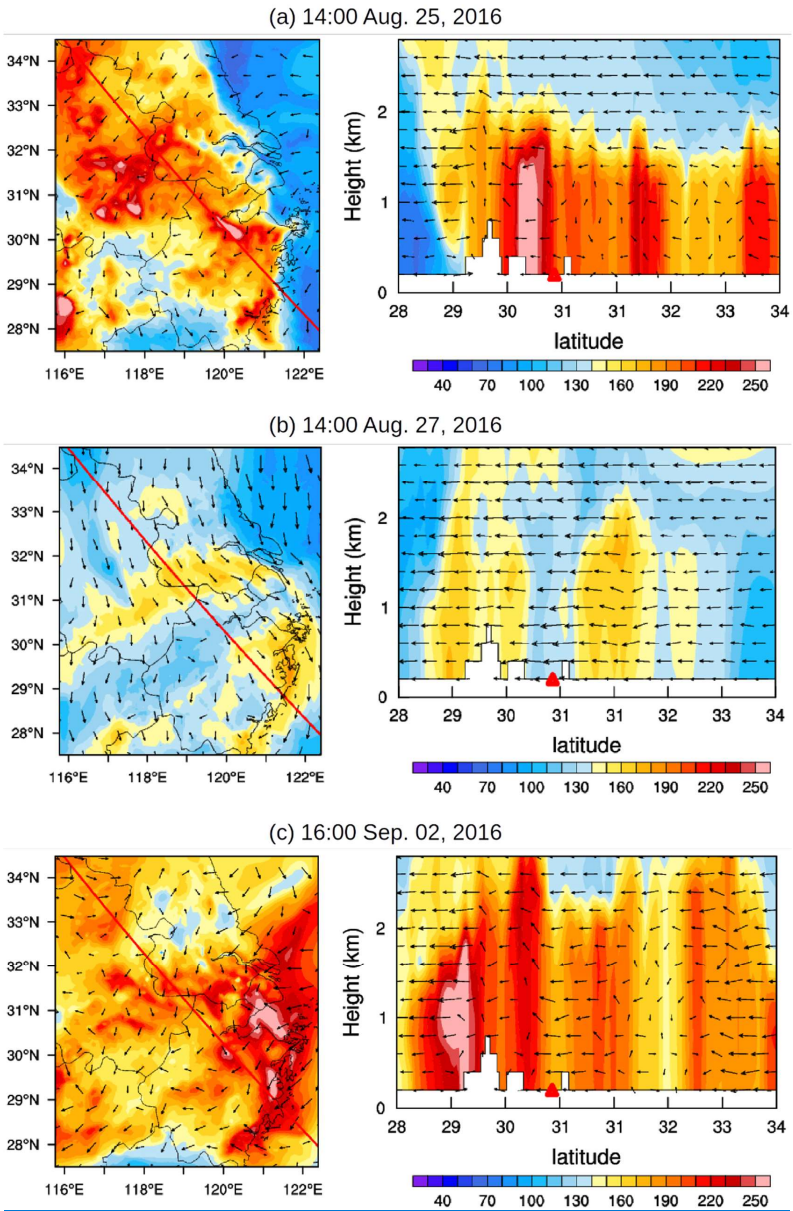

Fig. 67. Surface and ~~upper~~low-level O_3 distributions (μg m^{-3}) and wind fields (vectors, m s^{-1}) for representative episodes. (a) Stagnant weather before the tropical cyclone, (b) pollutant transport when the tropical cyclone approached, and (c) stagnant weather after the cyclone. The red line denotes the cross-section line of ~~upper~~low-level O_3 distributions. The red triangle denotes the location of Hangzhou.

Formatted: Font: (Asian) 等线, Font color: Auto
Formatted: Font: (Asian) 等线, Font color: Auto
Formatted: Font: (Asian) 等线
Formatted: Font: (Asian) 等线, Font color: Auto
Formatted: Font: (Asian) 等线
Formatted: Font: (Asian) 等线
Formatted: Font: (Asian) 等线
Formatted: Font: (Asian) 等线, Font color: Auto
Formatted: Font: (Asian) 等线
Formatted: Font: (Asian) Times New Roman, Font color: Auto

reactions dominate the ozone formation and accumulation. This phenomenon is consistent with the satellite-derived tropospheric O_3 distribution in the area (Su et al. 2017), and is also supported by the observed ozone data from the 96 sites in the YRD region as shown in Fig. 3c. During the 14-day emission control period of G20 summit, 52% of the observed ozone samples from the 96 sites are above the China's national level-II standard (160μg/m^3), suggesting that regional ozone pollution appears in the YRD region during the study period. As the cyclone approached on 27 August, a large belt of O_3 mass appeared in the upwind direction and moved toward Hangzhou under a prevailing north wind field (Fig. 7b). Regional pollutant transport may play an important role under this condition. However, because of the rain and cooling effects from the cyclone, the ozone concentration is relatively low in the whole YRD region.

3.53. Process analysis of O_3 formation

Formatted: Font color: Auto

Formatted: Font color: Auto

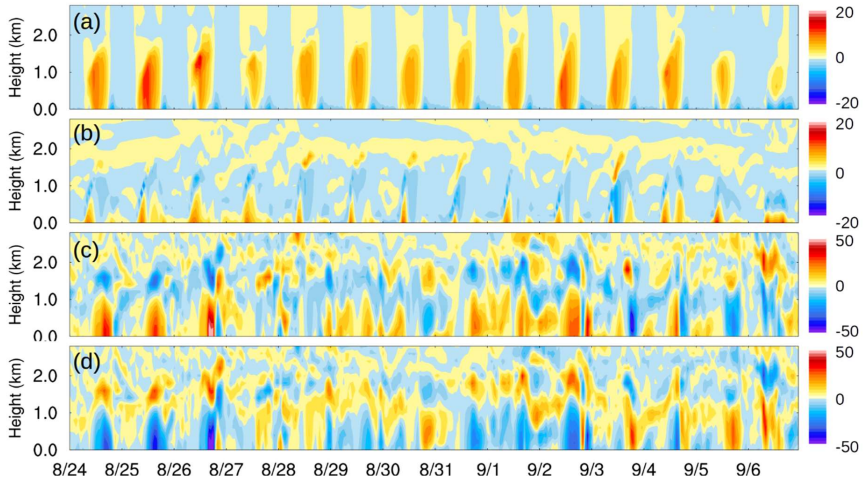

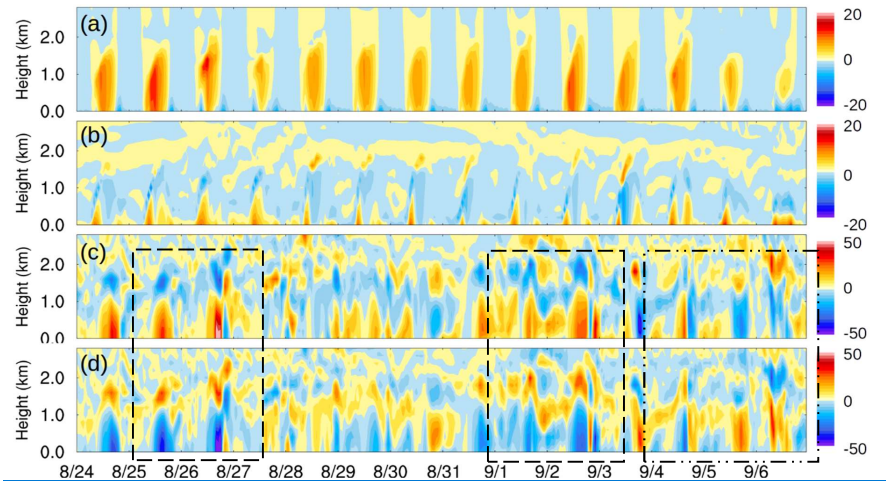

Fig. ~~7~~8. Hourly variations in the change rate of ~~upper~~low-level O_3 (ppb h^{-1}) ~~resulting~~resulted from (a) gas chemistry, (b) vertical diffusion, (c) horizontal advection, and (d) vertical advection in Hangzhou.

~~Four~~To further investigate the underlying mechanism of O_3 pollution, hourly ~~modeled~~variations in the change rate of low-level O_3 resulting from different physical and chemical processes ~~indicated the diurnal fluctuations in loops. Gas chemistry resulted~~ are presented in Fig.8. It is evident that gas chemistry is the dominant factor to the strong generation of ~~O_3 nearly above the upper-air height of 2 km~~ abundant O_3 in the entire planetary boundary layer (<2 km) in the daytime but ~~caused~~causes small amount of depletion of O_3 at the near-surface height (<0.3 km) in the nighttime (Fig. 8a). ~~7a).~~High concentration of O_3 diffuses from the upper layer ~~diffused~~ downward to the ground through vertical diffusion during the whole study period ~~but was significantly higher~~, which is obvious in the daytime (Fig. ~~7b). In addition~~8b). However, this effect is relatively weak compared to other processes. Horizontal and vertical advections seem to play more important roles in shaping the near-surface O_3, as indicated in ~~Fig~~Figs. 8c and ~~d, several~~8d. Several interesting dynamic O_3 circulations ~~were~~are observed between the near-surface and upper-air ~~heights during~~regions and indicated by the dashed boxes. During the periods of 24 ~~and 25~~-26 August and ~~on 02~~31 August to 2 September 2016~~. An~~, O_3-rich mass in the lower layer (<1 km) ~~traveled~~travels to Hangzhou through horizontal advection, and ~~it was~~is then transported ~~from the upper layer~~upward to the ~~high~~higher layer ~~(approximately 1.5 km)~~

Formatted: Font: (Asian) 等线, Font color: Auto
Formatted: Font: (Asian) 等线, Font color: Auto
Formatted: Font: (Asian) 等线
Formatted: Font: (Asian) 等线, Font color: Auto
Formatted: Font: (Asian) 等线
Formatted: Font: (Asian) PMingLiU
Formatted: Font: (Asian) Times New Roman, Font color: Auto
Formatted: First line: 0 ch
Formatted: Font: (Asian) 等线, Font color: Auto
Formatted: Font: (Asian) 等线, Font color: Auto
Formatted: Font: (Asian) 等线, Font color: Auto
Formatted: Font: (Asian) 等线, Font color: Auto
Formatted: Font: (Asian) 等线, Font color: Auto
Formatted: Font: (Asian) 等线, Font color: Auto
Formatted: Font: (Asian) 等线, Font color: Auto
Formatted: Font: (Asian) 等线
Formatted: Font: (Asian) 等线, Font color: Auto
Formatted: Font: (Asian) 等线, Font color: Auto
Formatted: Font: (Asian) 等线
Formatted: Font: (Asian) 等线, Font color: Auto
Formatted: Font: (Asian) 等线, Font color: Auto
Formatted: Font: (Asian) 等线, Font color: Auto
Formatted: Font: (Asian) 等线, Font color: Auto
Formatted: Font: (Asian) 等线, Font color: Auto
Formatted: Font: (Asian) 等线, Font color: Auto
Formatted: Font: (Asian) 等线, Font color: Auto
Formatted: Font: (Asian) 等线, Font color: Auto
Formatted: Font: (Asian) 等线, Font color: Auto
Formatted: Font: (Asian) 等线, Font color: Auto
Formatted: Font: (Asian) 等线, Font color: Auto
Formatted: Font: (Asian) 等线, Font color: Auto
Formatted: Font: (Asian) 等线, Font color: Auto
Formatted: Font: (Asian) 等线
Formatted: Font: (Asian) 等线, Font color: Auto
Formatted: Font: (Asian) 等线, Font color: Auto
Formatted: Font: (Asian) 等线, Font color: Auto
Formatted: Font: (Asian) 等线, Font color: Auto
Formatted: Font: (Asian) 等线, Font color: Auto

through vertical advection. ~~The mass subsequently reversed and traveled away from Hangzhou in the high~~At this higher layer ~~through horizontal advection in a circular manner. Urban heat island circulations caused the upward and downward flows.~~, the mass

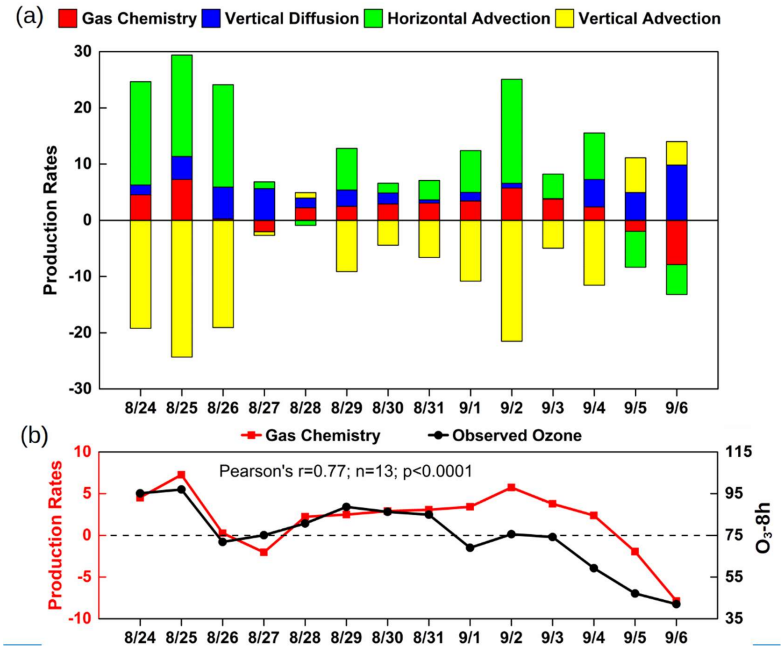

Formatted: Font: (Asian) 等线, Font color: Auto

Formatted: Font: (Asian) 等线, Font color: Auto

Formatted: Font: (Asian) 等线, Font color: Auto

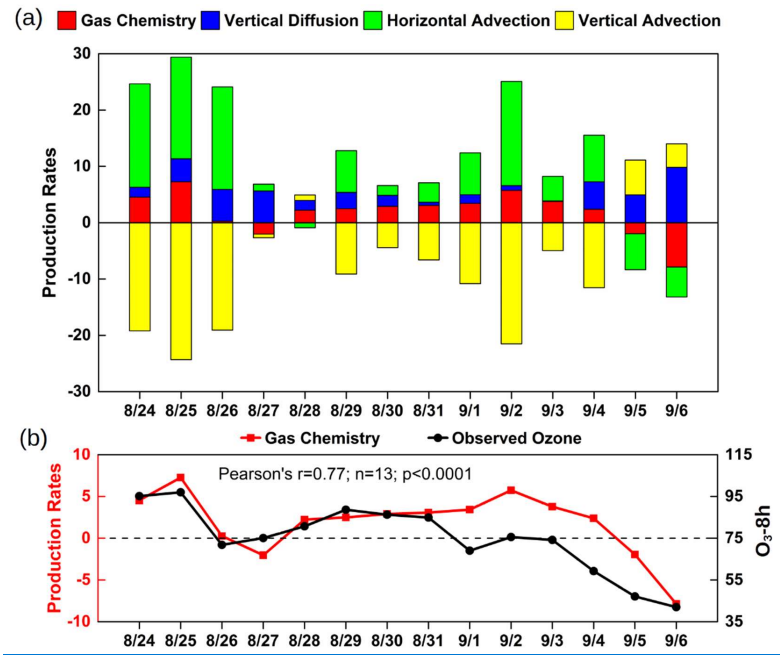

718

719 **Fig. 89.** (a) Daytime mean (08:00–17:00 LST) ~~variations in~~ change rate of simulated surface O_3 ~~change rate~~ (ppb

720 h^{-1}; left *y* axis) ~~resulting~~resulted from gas chemistry, vertical diffusion, ~~and~~ horizontal and vertical

721 ~~advection~~advections in Hangzhou. (b) ~~Comparison~~Correlation of daytime mean gas chemistry generation (ppb h^{-1};

722 left *y* axis) and observed surface-level maximum for daily ~~8 h~~8h concentration of O_3 (~~O_3-8h;~~ ppb; right *y* axis) in

723 Hangzhou. China's national level-II standard is approximately 75 ppb (160 μg m^{-3}).

724 ——subsequently travels away from Hangzhou to other places through horizontal advection in a

725 circular manner. This phenomenon might be associated with the urban heat island circulation (Lai

726 and Cheng, 2009). However, during the period of September 3-6 2016, similar circulation

727 phenomenon is observed, but the flow direction is reverse. The O_3-rich mass travels downward to the

728 ground through vertical advection and is then transported to surrounding regions through horizontal

729 advection. This downward circulation is also related to the meteorological conditions after the

730 cyclone. In addition, the horizontal and vertical advections of O_3 take on a chaotic status during

731 August 27-30, 2016, suggesting that complicated variable meteorological conditions happened in the

732 time. This is also the reason for the lower magnitude of diurnal variation in Stage 2.

Formatted: Font: (Asian) 等线, Font color: Auto
Formatted: Font: (Asian) 等线, Font color: Auto
Formatted: Font: (Asian) 等线
Formatted: Font: (Asian) PMingLiU
Formatted: Font: (Asian) 等线, Font color: Auto
Formatted: Font: (Asian) 等线, Font color: Auto
Formatted: Font: (Asian) PMingLiU
Formatted: Font: (Asian) 等线, Font color: Auto
Formatted: Font: (Asian) PMingLiU
Formatted: Font: (Asian) 等线, Font color: Auto
Formatted: Font: (Asian) PMingLiU
Formatted: Font: (Asian) PMingLiU
Formatted: Font: (Asian) PMingLiU
Formatted: Font: (Asian) PMingLiU
Formatted: Font: (Asian) 等线, Font color: Auto
Formatted: Font: (Asian) PMingLiU
Formatted: Font: (Asian) PMingLiU
Formatted: Font: (Asian) 等线, Font color: Auto
Formatted: Font: (Asian) PMingLiU
Formatted: Font: (Asian) 等线, Font color: Auto
Formatted: Font: (Asian) 等线
Formatted: Font: (Asian) Times New Roman, Font color: Auto
Formatted: Font: (Asian) 等线, Font color: Auto

Fig. 9 shows the daytime mean ~~variations~~change rate of simulated O_3 at the ground level resulted from various atmospheric processes ~~(Fig.~~ and the correlation of gas chemistry generation and observed maximum for daily 8h concentration of O_3. As a whole, the main sources of local surface ozone in Hangzhou are~~8a). Quantification of these variations revealed major positive contributions~~ from gas chemistry, vertical diffusion, and horizontal advection ~~to surface O_3 formation~~, with mean production rates of 1.9, 3.3, and 6.7 ppb h^{-1}, respectively, from ~~24 August to 06 September 2016. Firstly, the trends between~~August 24 to September 6, 2016, and the major sink is vertical advection. However, during some days such as September 5-6, the gas chemistry consumes O_3 while the vertical advection increases it. In general, strong net horizontal and vertical advections of O_3 are observed for most days of the period, except August 27-28 during

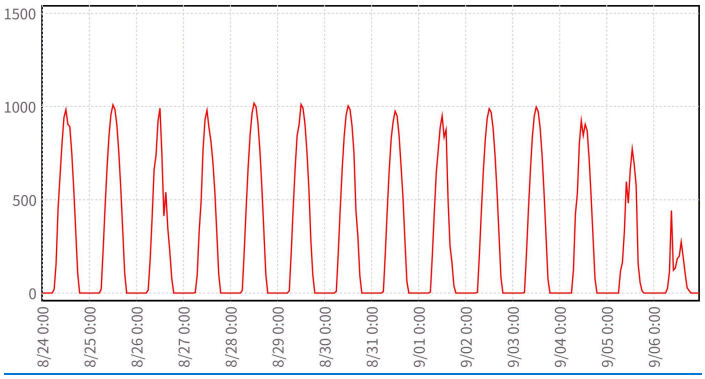

Fig. 10. Simulated hourly downward short wave flux at ground surface in Hangzhou (W m^{-2}) during August 24 to September 6, 2016.

which the strongest northwest cold winds (Fig. 4e) occurred and made the net advections of O_3 negligible. Similar to Fig. 8, dynamic O_3 circulations are observed for the periods of August 24-26, August 31 to September 2, and September 5-6. Particularly, the circular direction is reverse during September 5-6 and the net gas chemistry is to consume ozone due to weak solar radiation in the days as shown in Fig. 10.

In addition, the variation trend of the daytime mean ~~values associated with~~production rate of gas chemistry ~~and observed O_3-8h concentration were~~is consistent ~~(Fig.~~ with the observed MDA8

Formatted: Font: (Asian) 等线, Font color: Auto
Formatted: Font: (Asian) 等线
Formatted: Font: (Asian) 等线
Formatted: Font: (Asian) 等线, Font color: Auto
Formatted: Font: (Asian) PMingLiU
Formatted: Font: (Asian) 等线
Formatted: Font: (Asian) 等线
Formatted: Font: (Asian) 等线, Font color: Auto
Formatted: Font: (Asian) 等线
Formatted: Indent: First line: 0.85 cm
Formatted: Font: (Asian) 等线, Font color: Auto
Formatted: Font: (Asian) 等线, Font color: Auto
Formatted: Font: (Asian) 等线, Font color: Auto

concentration and the local chemical generation has large positive correlation (Pearson's r = 0.77) with the observed MDA8 concentrations (Fig. 8b~~), indicating~~). This indicates a trade-off effect among vertical diffusion ~~and~~, horizontal advection, and vertical advection. High O_3 concentrations (i.e., 25 August 2016 ~~O_3-8h~~MDA8: 98 ppb) ~~were~~are always accompanied by strong radiation and prolific generation of gas ~~chemicals. Local chemical generation was found to have large positive correlation (Pearson's r = 0.77) with O_3 concentrations. Secondly,~~chemical reactions. It is also interesting to find that vertical diffusion may ~~have~~ partially ~~compensated~~compensate for gas chemistry when the chemical reaction rate ~~was~~is relatively low or negative. For example, ~~on 26 and 27~~during August 26-27 and ~~05 and 06~~ September ~~2016, most of~~5-6, the vertical diffusion rates ~~were greater~~are higher than the chemical production rates. The low O_3 episode on these periods ~~mainly resulted~~may result from local chemical consumption. ~~Finally, advection processes were essential and integral to air circulation: horizontal advection exerted remarkably positive effects on surface O_3 concentrations in Hangzhou, and vertical advection exerted dispersion effects.~~

4. Discussion

The above results demonstrate that high ozone concentrations are observed, temporarily during most day time of the emission control period of G20 summit, and spatially in Hangzhou and even the whole YRD region, from the surface to the top of the planetary boundary layer. Strong horizontal and vertical advections appear, but they form circulations due to special meteorological conditions so that the effects of them almost cancel each other out. As a result, the serious ozone pollution in Hangzhou is mainly resultant from the local photochemical reactions. When the photochemical reactions are weak, the vertical diffusion from the upper-air notable background O_3 further compensates for the local surface ozone concentration. Therefore, it is of great importance to understand why the strict emission control measures make no obvious effect on the local photochemical reactions of ozone generation.

Chemical generation of O_3 is the net effect of photochemical generation and titration consumption. VOC oxidation (Jenkin et al., 1997; Sillman, 1999) in photochemical reactions provides

Formatted: Font: (Asian) 等线, Font color: Auto
Formatted: Font: (Asian) 等线, Font color: Auto
Formatted: Font: (Asian) 等线, Font color: Auto
Formatted: Font: (Asian) 等线, Font color: Auto
Formatted: Font: (Asian) 等线
Formatted: Font: (Asian) 等线, Font color: Auto
Formatted: Font: (Asian) 等线, Font color: Auto
Formatted: Font: (Asian) 等线, Font color: Auto
Formatted: Font: (Asian) 等线, Font color: Auto
Formatted: Font: (Asian) 等线, Font color: Auto
Formatted: Font: (Asian) 等线, Font color: Auto
Formatted: Font: (Asian) 等线, Font color: Auto
Formatted: Font: (Asian) 等线, Font color: Auto
Formatted: Font: (Asian) 等线, Font color: Auto
Formatted: Font: (Asian) 等线, Font color: Auto
Formatted: Font: (Asian) 等线, Font color: Auto
Formatted: Font: (Asian) 等线
Formatted: Font: (Asian) 等线, Font color: Auto
Formatted: Font: (Asian) 等线, Font color: Auto
Formatted: Font: (Asian) 等线, Font color: Auto
Formatted: Justified, Line spacing: Double
Formatted: Font: (Asian) 等线, Font color: Auto
Formatted: Font: (Asian) 等线
Formatted: Font: (Asian) 等线, Font color: Auto
Formatted: Font: (Asian) PMingLiU

779 critical oxidants (i.e., RO_2) that efficiently convert NO to NO_2, resulting in further accumulation of
780 O_3 (Wang et al., 2017). ~~This study revealed notable background O_3 concentrations in the upper-air~~
781 ~~layer in the YRD region. Peripheral downdrafts in large-scale cyclone circulation can transport an~~
782 ~~O_3-rich mass in the upper troposphere or lower stratosphere downward to the surface (Tang et al.,~~
783 ~~2011; Hsu and Prather, 2014). This type of O_3 intrusion during this period was reported in southeast~~
784 ~~China (Ni et al.,~~The chemical generation of O3 is controlled by NO_x and VOCs depending on which
785 substance is lack in the reactions. As a consequence, there are two sensitivity regimes of O_3
786 production, namely, the NO_x-limited and VOC-limited regimes. Previous studies have shown that the
787 sensitivity pattern of surface O_3 formation in Hangzhou is dominant by the VOCs-limited regime
788 (Yan *et al.* 2016; Li *et al.*, 2017; Su *et al.*, 2017). In this regime, if the regional reduction of VOCs is
789 much higher than that of NO_x, the O_3 concentration can be reduced, otherwise if the regional reduction
790 of VOCs is much less than that of NO_x, the inhibitory effect of NO_x on O_3 generation will be
791 weakened, and the O_3 concentration will increase remarkably (Wang et al. 2015). According to the
792 studies of Su et al. (2017), Zheng et al. (2019), and Wu et al. (2019), it can be deduced that NO_x has
793 been significantly reduced by about 60%, at least two times of the reduction of VOCs in Hangzhou.
794 The influence of stringent emission control measures on VOCs is not as immediate and effect as that
795 on NO_x, which is associated with the fact that there was a large amount of biogenic VOC emission in
796 Hangzhou and surrounding regions (Liu et al. 2018; Wu et al. 2020). In fact, the average temperature
797 during the study period is as high as around 31°C (Fig. 4c), which facilitates the biogenic VOC
798 emissions and photochemical reactions. As a result, the photochemical generation of O_3 was not under
799 control and high concentration of ozone appeared. However, it is worth noting that after the emergent
800 VOCs control measures had been implemented in the area during the third stage, the net generation
801 rate of O_3 gradually reduces since September 2, 2016, leading to a period of relatively low ozone
802 concentration together with other meteorological effects. These discussions implicate that to alleviate
803 ozone pollution, the ratio of reduction of VOCs to that of NO_x is the key parameter based on the O_3-
804 NO_x-VOCs sensitivity analysis. As the biogenic VOCs are important sources of the total VOCs in the

Formatted: Font: (Asian) 等线, Font color: Auto
Formatted: Font: (Asian) 等线
Formatted: Font: (Asian) 等线, Font color: Auto
Formatted: Font: (Asian) 等线
Formatted: Font: (Asian) 等线, Font color: Auto
Formatted: Font: (Asian) PMingLiU
Formatted: Font: (Asian) 等线, Font color: Auto

YRD region, it is necessary to balance the reduction of NO_x to make the ratio within effective regime in the future.

~~–2019). Based on our results, we inferred that a considerably high background O_3 concentration in the upper air markedly contributed to surface O_3 pollution; this inference agreed (hemispheric background) with the findings of studies conducted in Europe (Wilson et al., 2012) and the United States (Lin et al., 2012, 2015).~~

~~We demonstrated that local chemical generation in Hangzhou was enhanced during episodes of high O_3 concentrations before and after the tropical cyclone that occurred during the study period. Chemical generation of O_3 is the net effect of photochemical generation and titration consumption. VOC oxidation (Jenkin et al., 1997; Sillman, 1999) in photochemical reactions provides critical oxidants (i.e., RO_2) that efficiently convert NO to NO_2, resulting in further accumulation of O_3 (Wang et al., 2017). In the present study, downward shortwave flux at the ground level (Fig. S3) was more intense on days with high O_3 concentrations than on those with low O_3 concentrations. This strong solar radiation strengthened O_3 photochemical generation. In addition to the stagnant weather conditions, air subsidence in peripheral circulations of tropical cyclones helps to trap heat and pollutants at the surface (Jiang et al., 2015; Shu et al., 2016). Furthermore, a tropical system with calm, hot dry weather favors the development of an urban heat island, which causes thermal circulations as well as the convergence of the surrounding O_3 and its precursors (Lai and Cheng, 2009). The increased temperature also accelerates the photochemical reactions (Narumi et al., 2009; Walcek et al., 1995). In the present study, these enhanced photochemistry processes dominated O_3 chemical generation, resulting in high O_3 concentrations. This result was consistent with the results of a previous field study (Su et al., 2017). Low-level O_3 episodes (i.e., 06 September) in Hangzhou were accompanied by a rain band in the YRD region. Rain band–related cumulus clouds blocked solar radiation, thereby weakening O_3 photochemical generation. Consequently, titration consumption dominated the chemical generation process, resulting in low or negative O_3 chemical production.~~

Formatted: Font color: Auto

Formatted: Font: (Asian) 等线, Font color: Auto

Formatted: Font: (Asian) 等线

Formatted: Font: (Asian) 等线, Font color: Auto

Formatted: Font: (Asian) PMingLiU

Formatted: Font: (Asian) 等线, Font color: Auto

Formatted: Font: (Asian) 等线

Formatted: Font: (Asian) 等线, Font color: Auto

Formatted: Font: (Asian) PMingLiU

Formatted: Font: (Asian) 等线, Font color: Auto

5. Conclusions

~~Changes in O_3 concentrations in Hangzhou~~ To understand the unique response of ozone to short-term emission control measures during the G20 summit ~~were well represented~~in Hangzhou, the spatial-temporal characteristics and process analysis of O_3 pollution are investigated by using the WRF-Chem model. Statistical evaluations of meteorological and chemical parameters ~~suggested~~suggest that the model system ~~results satisfactorily matched~~is able to reasonably predict the observed data for both the ground and upper-air levels in MICS-~~ASIA~~Asia III. ~~The model results revealed that the O_3~~High ozone concentrations are observed, temporarily during most day time of the emission control period of G20 summit, and spatially in Hangzhou ~~were highly related to a tropical cyclone over the East China Sea. Throughout the simulation period, large-scale air mass~~and even the whole YRD region, from the surface to the top of the planetary boundary layer. Horizontal and vertical advection circulations ~~and energy transport~~are captured in Hangzhou, with horizontal advection the source and vertical advection the sink of the surface O_3 in Hangzhou. Consequently, the serious ozone pollution is mainly resultant from the local photochemical reactions which are not under good control by the ~~tropical cyclone probably caused the high~~emission reduction measures. As the surface O_3 formation in Hangzhou is dominant by the VOCs-limited regime, the significant reduction of NO_x compared to that of VOCs is unfavorable to chemical generation of O_3. The ratio of reduction of VOCs to that of NO_x based on the O_3-NO_x-VOCs sensitivity analysis is a critical parameter for reduction of ozone formation from photochemical reactions. In addition, it is found that the vertical diffusion from the upper-air ~~O_3-rich mass in the horizontal and vertical scales of the YRD region; this phenomenon engendered a negative~~notable background O_3 also plays an important role in shaping the surface ozone concentration~~. As the tropical cyclone approached, bringing with it a prevailing north wind component, Hangzhou was affected by pollutant transport from North China. After or before the tropical cyclone, peripheral downdraft or air subsidence produced stable and calm weather, with high pressure and temperature and~~ when the photochemical reactions are weak ~~wind, and the urban heat island effect was aggravated. The combination of these conditions enhanced the~~

Formatted: Font color: Auto
Formatted: Font: (Asian) 等线, Font color: Auto
Formatted: Font: (Asian) PMingLiU
Formatted: Font: (Asian) PMingLiU
Formatted: Font: (Asian) 等线, Font color: Auto
Formatted: Font: (Asian) PMingLiU
Formatted: Font: (Asian) 等线, Font color: Auto
Formatted: Font: (Asian) 等线
Formatted: Font: (Asian) 等线
Formatted: Font: (Asian) PMingLiU
Formatted: Font: (Asian) PMingLiU
Formatted: Font: (Asian) PMingLiU
Formatted: Font: (Asian) PMingLiU
Formatted: Font: (Asian) PMingLiU
Formatted: Font: (Asian) 等线, Font color: Auto
Formatted: Font: (Asian) 等线, Font color: Auto
Formatted: Font: (Asian) PMingLiU

~~chemical generation process, resulting in a marked increase in surface O_3 concentrations. Our study provides scientific insight into urban O_3 formation and dispersion under conditions where short-term emission reduction measures had been applied in East China during a tropical cyclone event.~~

Author contribution

Zhizhen Ni: Data curation, Investigation, Writing - original draft. **Kun Luo:** Methodology, Resources, Writing - review & editing, Supervision. **Yang Gao:** Formal analysis, Methodology, Writing - review & editing. **Xiang Gao:** Data curation, Resources. **Fei Jiang:** Methodology, Writing - review & editing. **Cheng Huang:** Data curation, Formal analysis. **Jianren Fan:** Resources, Supervision. **Joshua Fu**: Writing - review & editing. **Changhong Chen**: Formal analysis.

Acknowledgments

This work was financially supported by special funds from the Ministry of Environmental Protection of China (No. 201409008-4) and the Zhejiang Provincial Key Science and Technology Project for Social Development (No. 2014C03025). We would like to thank the US National Oceanic and Atmospheric Administration for its technical support in WRF-Chem modeling. High-resolution emission inventories were provided by the Institute of Environmental Science, Shanghai, China, and the official documents of emission control policies were obtained from the Hangzhou Environmental Monitoring Center.

~~Reference~~

Formatted: Font: (Asian) 等线, Font color: Custom Color(RGB(34,34,34)), Condensed by 0.05 pt, Pattern: Clear (White)

Formatted: First line: 0 ch

Formatted: Font color: Auto

Formatted: Font: (Asian) 等线, Not Bold, Font color: Auto

Formatted: Font: (Asian) 等线, Font color: Auto

Formatted: Default Paragraph Font

Formatted: Default Paragraph Font, Font color: Auto

Competing interests

The authors declare that they have no conflict of interest.

References

Browell, E.V., Ismail, S., Grant, W.B.: Differential absorption lidar (DIAL) measurements from air and space, Appl. Phys. B Lasers Opt, 67, 399–410, https://doi.org/10.1007/s003400050523, 1998.

Browell, E. V.: Differential Absorption Lidar Sensing of Ozone, Proc. IEEE, 77, 419–432, https://doi.org/10.1109/5.24128, 1989

Brown, J.F., Loveland, T.R., Merchant, J.W., Reed, B.C., Ohlen, D.O.: Using Multisource Data in Global Land-Cover Characterization - Concepts, Requirements, and Methods, Photogramm. Eng. Remote Sensing, 59, 977–987, 1993.

Calfapietra, C., Morani, A., Sgrigna, G., Di Giovanni, S., Muzzini, V., Pallozzi, E., Guidolotti, G., Nowak, D., Fares, S.: Removal of Ozone by Urban and Peri-Urban Forests: Evidence from Laboratory, Field, and Modeling Approaches, J. Environ. Qual, 45, 224, https://doi.org/10.2134/jeq2015.01.0061, 2016.

Cheng, W.L., Lai, L.W., Den, W., Wu, M.T., Hsueh, C.A., Lin, P.L., Pai, C.L., Yan, Y.L.: The relationship between typhoons' peripheral circulation and ground-level ozone concentrations in central Taiwan, Environ. Monit. Assess, 186, 791–804, https://doi.org/10.1007/s10661-013-3417-7, 2014.

Emery, C., Tai, E., Yarwood, G.: Enhanced meteorological modeling and performance evaluation for two Texas episodes, International Corp (Ed.), Report to the Texas Natural Resources Conservation Commission, p.b.E (2001) [Novato, CA.], 2001

Emmons, L.K., Walters, S., Hess, P.G., Lamarque, J.-F., Pfister, G.G., Fillmore, D., Granier, C., Guenther, A., Kinnison, D., Laepple, T., Orlando, J., Tie, X., Tyndall, G., Wiedinmyer, C., Baughcum, S.L., Kloster, S.: Description and evaluation of the Model for Ozone and Related chemical Tracers, version 4 (MOZART-4), Geosci. Model Dev., 3, 43–67, https://doi.org/10.5194/gmd-3-43-2010, 2010.

Friedl, M. ., McIver, D. ., Hodges, J. C. ., Zhang, X. ., Muchoney, D., Strahler, A. ., Woodcock, C. ., Gopal, S., Schneider, A., Cooper, A., Baccini, A., Gao, F. and Schaaf, C.: Global land cover mapping from MODIS: algorithms and early results, Remote Sens. Environ., 83(12), 287–302, https://doi.org/10.1016/S0034-4257(02)00078-0, 2002.

Formatted: Font: (Asian) 等线, Font color: Auto

Formatted: Justified

Formatted

Gao, J., Zhu, B., Xiao, H., Kang, H., Hou, X., Shao, P.: A case study of surface ozone source apportionment during a high concentration episode, under frequent shifting wind conditions over the Yangtze River Delta, China, Sci. Total Environ, 544, 853–863, https://doi.org/10.1016/j.scitotenv.2015.12.039, 2016.

Gonçalves, M., Jiménez-Guerrero, P., Baldasano J.M.: Contribution of atmospheric processes affecting the dynamics of air pollution in South-Western Europe during a typical summertime photochemical episode, Atmos. Chem. Phys, 9, 849–864, https://doi.org/10.5194/acp-9-849-2009, 2009.

Grell, G.A., Peckham, S.E., Schmitz, R., McKeen, S.A., Frost, G., Skamarock, W.C., Eder, B. Fully coupled "online" chemistry within the WRF model, Atmos. Environ., 39, 6957–6975, https://doi.org/10.1016/j.atmosenv.2005.04.027, 2005.

Grell, G., Baklanov, A.: Integrated modeling for forecasting weather and air quality: A call for fully coupled approaches, Atmos. Environ., 45, 6845–6851, https://doi.org/10.1016/j.atmosenv.2011.01.017, 2011.

Haiwei Li, Dongfang Wang, Long Cui, Yuan Gao, Juntao Huo, Xinning Wang, Zhuozhi Zhang, Yan Tan, Yu Huang, Junji Cao, Judith C. Chow, Shun-cheng Lee, Qingyan Fu. Characteristics of atmospheric PM2.5 composition during the implementation of stringent pollution control measures in shanghai for the 2016 G20 summit. Science of the Total Environment 648 (2019) 1121?1129

Ha, S., Hu, H., Roussos-Ross, D., Haidong, K., Roth, J., Xu, X.: The effects of air pollution on adverse birth outcomes, Environ. Res., 134, 198–204, https://doi.org/10.1016/j.envres.2014.08.002, 2014.

~~Hsu, J., Prather, M.J.: Is the residual vertical velocity a good proxy for stratosphere-troposphere exchange of ozone?, Geophys. Res. Lett., 41, 9024–9032, https://doi.org/10.1002/2014GL061994, 2014.~~

Huang, J.P., Fung, J.C.H., Lau, A.K.H., Qin, Y.: Numerical simulation and process analysis of typhoon-related ozone episodes in Hong Kong, J. Geophys. Res. D Atmos., 110, 1–17, https://doi.org/10.1029/2004JD004914, 2005.

Huang, C., Chen, C. H., Li, L., Cheng, Z., Wang, H. L., Huang, H. Y., Streets, D. G., Wang, Y. J., Zhang, G. F. and Chen, Y. R.: Emission inventory of anthropogenic air pollutants and VOC species in the Yangtze River Delta region, China, Atmos. Chem. Phys., https://doi.org/10.5194/acp-11-4105-2011, 2011.

Huan Yu, Wei Dai, Lili Ren, Dan Liu, Xintian Yan, Hang Xiao, Jun He, Honghui Xu. The Effect of Emission Control on the Submicron Particulate Matter Size Distribution in Hangzhou during the 2016 G20 Summit. Aerosol and Air Quality Research, 18: 2038–2046, 2018.

Hung, C.H., LouoC, K.: Relationships between Ambient Ozone Concentration Changes in Southwestern Taiwan and Invasion Tracks of Tropical Typhoons, Adv. Meteorol., https://doi.org/10.1155/2015/402976, 2015.

Formatted: Font: (Asian) 等线, Font color: Auto

Formatted: Justified

Formatted: Font: (Asian) 等线, Font color: Auto

Formatted: Font: (Asian) 等线, Font color: Auto

Formatted: Justified

Formatted: Font: (Asian) 等线, Font color: Auto

Formatted: Justified

Hu S.W., Wu, X.F., Luo K., Gao, X. and Fan, J.R. (2015). Source apportionment of air pollution in Hangzhou city based on CMAQ. Energy Eng. 7: 40–44.

Jenkin, M. E., Saunders, S. M. and Pilling, M. J.: The tropospheric degradation of volatile organic compounds: A protocol for mechanism development, Atmos. Environ., 31(1), 81–104, https://doi.org/10.1016/S1352-2310(96)00105-7, 1997.

Jfffries H. E., Tonnesen S.: A comparison of two photochemical reaction mechanisms using mass balance and process analysis, Atmospheric Environment, 28(18), 2991-3003, 1994.

Jiang, F., Zhou, P., Liu, Q., Wang, T., Zhuang, B., Wang, X.: Modeling tropospheric ozone formation over East China in springtime, J. Atmos. Chem., 69, 303–319, https://doi.org/10.1007/s10874-012-9244-3, 2012.

Jiang, Y.C., Zhao, T.L., Liu, J., Xu, X.D., Tan, C.H., Cheng, X.H., Bi, X.Y., Gan, J.B., You, J.F., Zhao, S.Z.: Why does surface ozone peak before a typhoon landing in southeast China?, Atmos. Chem. Phys., 15, 13331–13338, https://doi.org/10.5194/acp-15-13331-2015, 2015.

Ji, Y., Qin, X., Wang, B., Xu, J., Shen, J., Chen, J., Huang, K., Deng, C., Yan, R., Xu, K. and Zhang, T. (2018). Counteractive effects of regional transport and emission control on the formation of fine particles: A case study during the Hangzhou G20 summit, Atmos. Chem. Phys. 18: 13581–13600.

Jones, S.L., Creighton, G.A., Kuchera, E.L., Rentschler, S.A.: Adapting WRF-CHEM GOCART for Fine-Scale Dust Forecasting, in: AGU Fall Meeting Abstracts, p. 6., 2011.

Kai Wu, Ping Kang, Xin Tie, Shan Gu, Xiaoling Zhang, Xiaohang Wen, Lingkai Kong, Sihui Wang, Yuzi Chen, Weihao Pan, Zhanshan Wang. Evolution and Assessment of the Atmospheric Composition in Hangzhou and its Surrounding Areas during the G20 Summit. Aerosol and Air Quality Research, 19: 2757–2769, 2019

Kalnay, E., M. Kanamitsu, R. Kistler, W. Collins, D. Deaven, L. Gandin, M. Iredell, S. Saha, G. White, J. Woollen, Y. Zhu, M. Chelliah, W. Ebisuzaki, W. Higgins, J. Janowiak, K.C. Mo, C. Ropelewski, J. Wang, A. Leetmaa, R. Reynolds, R. Jenne, and D. Joseph: The NCEP/NCAR 40-Year Reanalysis Project, Bull. Amer. Meteor. Soc., 77, 437–472, https://doi.org/10.1175/1520-0477(1996)077<0437:TNYRP>2.0.CO;2, 1996.

Kheirbek, I., Wheeler, K., Walters, S., Kass, D., Matte, T.: PM2.5 and ozone health impacts and disparities in New York City: Sensitivity to spatial and temporal resolution, Air Qual. Atmos. Heal., 6, 473–486, https://doi.org/10.1007/s11869-012-0185-4, 2013.

Knote, C., Tuccella, P., Curci, G., Emmons, L., Orlando, J.J., Madronich, S., Baró, R., Jiménez-Guerrero, P., Luecken, D., Hogrefe, C., Forkel, R., Werhahn, J., Hirtl, M., Pérez, J.L., San José, R., Giordano, L., Brunner, D., Yahya, K., Zhang, Y.: Influence of the choice of gas-phase mechanism on predictions of key gaseous

Formatted: Font: (Asian) 等线, Font color: Auto
Formatted: Justified
Formatted: Font: (Asian) 等线, Font color: Auto
Formatted: Justified
Formatted: Font: (Asian) 等线, Font color: Auto
Formatted: Font: (Asian) 等线, Font color: Auto
Formatted: Justified
Formatted: Font: (Asian) 等线, Font color: Auto
Formatted: Justified

pollutants during the AQMEII phase-2 intercomparison, Atmos. Environ., 115, 553–568, https://doi.org/10.1016/j.atmosenv.2014.11.066, 2015.

Lai, L. W. and Cheng, W. L.: Air quality influenced by urban heat island coupled with synoptic weather patterns, Sci. Total Environ., 407(8), 2724–2733, https://doi.org/10.1016/j.scitotenv.2008.12.002, 2009.

Landry, J.S., Neilson, E.T., Kurz, W.A., Percy, K.E.: The impact of tropospheric ozone on landscape-level merchantable biomass and ecosystem carbon in Canadian forests, Eur. J. For. Res., 132, 71–81, https://doi.org/10.1007/s10342-012-0656-z, 2013.

~~Lelieveld, J., Evans, J.S., Fnais, M., Giannadaki, D., Pozzer, A.: The contribution of outdoor air pollution sources to premature mortality on a global scale, Nature, 525, 367–71, https://doi.org/10.1038/nature15371, 2015.~~

Li, J., Nagashima, T., Kong, L., Ge, B., Yamaji, K., Fu, J. S., Wang, X., Fan, Q., Itahashi, S., Lee, H.-J., Kim, C.-H., Lin, C.-Y., Zhang, M., Tao, Z., Kajino, M., Liao, H., Li, M., Woo, J.-H., Kurokawa, J.-I., Wu, Q., Akimoto, H., Carmichael, G. R., and Wang, Z.: Model evaluation and inter-comparison of surface-level ozone and relevant species in East Asia in the context of MICS-Asia phase III Part I: overview, Atmos. Chem. Phys. Discuss., https://doi.org/10.5194/acp-2018-1283, in review, 2019.

Li, K., Chen, L., Ying, F., White, S.J., Jang, C., Wu, X., Gao, X., Hong, S., Shen, J., Azzi, M. and Cen, K. (2017). Meteorological and chemical impacts on ozone formation: A case study in Hangzhou, China. Atmos. Res. 196: 40–52.

Li, L., Chen, C. H., Fu, J. S., Huang, C., Streets, D. G., Huang, H. Y., Zhang, G. F., Wang, Y. J., Jang, C. J., Wang, H. L., Chen, Y. R. and Fu, J. M.: Air quality and emissions in the Yangtze River Delta, China, Atmos. Chem. Phys., https://doi.org/10.5194/acp-11-1621-2011, 2011.

Li, M., Song, Y., Huang, X., Li, J., Mao, Y., Zhu, T., Cai, X. and Liu, B.: Improving mesoscale modeling using satellite-derived land surface parameters in the Pearl River Delta region, China, J. Geophys. Res. Atmos., 119(11), 6325–6346, https://doi.org/10.1002/2014JD021871, 2014.

Li, M., Zhang, Q., Kurokawa, J.-I., Woo, J.-H., He, K., Lu, Z., Ohara, T., Song, Y., Streets, D.G., Carmichael, G.R., Cheng, Y., Hong, C., Huo, H., Jiang, X., Kang, S., Liu, F., Su, H., Zheng, B.: MIX: a mosaic Asian anthropogenic emission inventory under the international collaboration framework of the MICS-Asia and HTAP, Atmos. Chem. Phys., 17, 935–963, https://doi.org/10.5194/acp-17-935-2017, 2017.

Lin, M., Fiore, A.M., Cooper, O.R., Horowitz, L.W., Langford, A.O., Levy, H., Johnson, B.J., Naik, V., Oltmans, S.J., Senff, C.J.: Springtime high surface ozone events over the western United States: Quantifying the role of stratospheric intrusions, J. Geophys. Res. Atmos., 117, https://doi.org/10.1029/2012JD018151, 2012.

Formatted: Font: (Asian) 等线, Font color: Auto

Formatted: Justified

Formatted: Font: (Asian) 等线

Formatted: Font: (Asian) 等线, Font color: Auto

Formatted: Justified

Formatted: Font: (Asian) 等线, Font color: Auto

Lin, M., Fiore, A.M., Horowitz, L.W., Langford, A.O., Oltmans, S.J., Tarasick, D., Rieder, H.E.: Climate variability modulates western US ozone air quality in spring via deep stratospheric intrusions, Nat. Commun., 6, 7105, https://doi.org/10.1038/ncomms8105, 2015.

Liu, H., Ma, W., Qian, J., Cai, J., Ye, X., Li, J. and Wang, X. (2015). Effect of urbanization on the urban meteorology and air pollution in Hangzhou. J. Meteorol. Res. 29: 950–965.

Liu, Y., Li, L., An, J., Huang, L., Yan, R., Huang, C., Wang, H., Wang, Q., Wang, M. and Zhang, W.: Estimation of biogenic VOC emissions and its impact on ozone formation over the Yangtze River Delta region, China, Atmos. Environ., https://doi.org/10.1016/j.atmosenv.2018.05.027, 2018.

McNally DE: 12 km MM5 performance goals, Presentation to the Ad-hov Meteorology Group, 2009.

Monks, P.S., Archibald, A.T., Colette, A., Cooper, O., Coyle, M., Derwent, R., Fowler, D., Granier, C., Law, K.S., Mills, G.E., Stevenson, D.S., Tarasova, O., Thouret, V., von Schneidemesser, E., Sommariva, R., Wild, O., Williams, M.L.: Tropospheric ozone and its precursors from the urban to the global scale from air quality to short-lived climate forcer, Atmos. Chem. Phys., 15, 8889–8973, https://doi.org/10.5194/acp-15-8889-2015, 2015.

Nagashima, T., Sudo, K., Akimoto, H., Kurokawa, J., Ohara, T., 2017. Long-term change in the source contribution to surface ozone over Japan. Atmos. Chem. Phys. 17, 8231–8246, https://doi.org/10.5194/acp-17-8231-2017

~~Narumi, D., Kondo, A. and Shimoda, Y.: The effect of the increase in urban temperature on the concentration of photochemical oxidants, Atmos. Environ., 43(14), 2348–2359, https://doi.org/10.1016/j.atmosenv.2009.01.028, 2009.~~

Ni, Z. zhen, Luo, K., Zhang, J. xi, Feng, R., Zheng, H. xin, Zhu, H. ran, Wang, J. fan, Fan, J. ren, Gao, X. and Cen, K. fa: Assessment of winter air pollution episodes using long-range transport modeling in Hangzhou, China, during World Internet Conference, 2015, in Environmental Pollution, vol. 236, pp. 550–561., 2018.

Ni, Z. zhen, Luo, K., Gao, X., Gao, Y., Fan, J. ren, Fu, Joshua S. Cen, C.,: Exploring the stratospheric source of ozone pollution over China during the 2016 Group of Twenty summit, 2019, Atmospheric Pollution Research, https://doi.org/10.1016/j.apr.2019.02.010

Paoletti, E., De Marco, A., Beddows, D.C.S., Harrison, R.M., Manning, W.J.: Ozone levels in European and USA cities are increasing more than at rural sites, while peak values are decreasing, Environ. Pollut., 192, 295–299, https://doi.org/10.1016/j.envpol.2014.04.040, 2014.

Formatted: Font: (Asian) 等线

Formatted: Justified

Formatted: Font: (Asian) 等线, Font color: Auto

Formatted: Font: (Asian) 等线, Font color: Auto

Formatted: Font: (Asian) 等线, Font color: Auto

Formatted: Justified

Shanshan Zheng, Xiaofeng Xu, Yunjiang Zhang, Lingrui Wang, Yifan Yang, Shiguang Jin, Xiaoxiao Yang. Characteristics and sources of VOCs in urban and suburban environments in Shanghai, China, during the 2016 G20 summit. Atmospheric Pollution Research 10 (2019) 1766?1779

Shi, C., Wang, S., Liu, R., Zhou, R., Li, D., Wang, W., Li, Z., Cheng, T., Zhou, B.: A study of aerosol optical properties during ozone pollution episodes in 2013 over Shanghai, China, Atmos. Res., 153, 235–249, https://doi.org/10.1016/j.atmosres.2014.09.002, 2015.

Shu, L., Xie, M., Wang, T., Chen, P., Han, Y., Li, S., Zhuang, B., Li, M., Gao, D.: Integrated studies of a regional ozone pollution synthetically affected by subtropical high and typhoon system in the Yangtze River Delta region, China, Atmos. Chem. Phys. Discuss., 0, 1–32, https://doi.org/10.5194/acp-2016-581, 2016.

Sillman, S.: The relation between ozone, NO(x) and hydrocarbons in urban and polluted rural environments, Atmos. Environ., 33(12), 1821–1845, https://doi.org/10.1016/S1352-2310(98)00345-8, 1999.

Stauffer, D.R., Seaman, N.L., Binkowski, F.S.: Use of Four-Dimensional Data Assimilation in a Limited-Area Mesoscale Model Part II: Effects of Data Assimilation within the Planetary Boundary Layer, Mon. Weather Rev., https://doi.org/10.1175/1520-0493(1991)119<0734:UOFDDA>2.0.CO;2, 1991.

Su, W., Liu, C., Hu, Q., Fan, G., Xie, Z., Huang, X., Zhang, T., Chen, Z., Dong, Y., Ji, X., Liu, H., Wang, Z., Liu, J.: Characterization of ozone in the lower troposphere during the 2016 G20 conference in Hangzhou, Sci. Rep., 7, 17368, https://doi.org/10.1038/s41598-017-17646-x, 2017.

Tang, G., Li, X., Wang, Y., Xin, J., Ren, X.: Surface ozone trend details and interpretations in Beijing, 2001 – 2006, Atmos. Chem. Phys., 8813–8823, https://doi.org/10.5194/acpd-9-8159-2009, 2009.

Tang, G., Wang, Y., Li, X., Ji, D., Hsu, S., Gao, X.: Spatial-temporal variations in surface ozone in Northern China as observed during 2009-2010 and possible implications for future air quality control strategies, Atmos. Chem. Phys., 12, 2757–2776, https://doi.org/10.5194/acp-12-2757-2012, 2012.

Tang, G., Zhu, X., Xin, J., Hu, B., Song, T., Sun, Y., Wang, L., Cheng, M., Li, X., Wang, Y., Zhang, J., Chao, N., Kong, L., Li, X.: Modelling study of boundary-layer ozone over northern China - Part I: Ozone budget in summer, Atmos. Res., 187, 128–137, https://doi.org/10.1016/j.atmosres.2016.10.017, 2017a.

~~Tang, Q., Prather, M.J., Hsu, J.: Stratosphere-troposphere exchange ozone flux related to deep convection, Geophys. Res. Lett., 38, https://doi.org/10.1029/2010GL046039, 2011.~~

Teixeira, E., Fischer, G., van Velthuizen, H., van Dingenen, R., Dentener, F., Mills, G., Walter, C., Ewert, F.: Limited potential of crop management for mitigating surface ozone impacts on global food supply, Atmos. Environ., 45, 2569–2576, https://doi.org/10.1016/j.atmosenv.2011.02.002, 2011.

Formatted: Font: (Asian) 等线, Font color: Auto

Formatted: Justified

Formatted: Font: (Asian) 等线, Font color: Auto

Formatted: Font: (Asian) 等线, Font color: Auto

Formatted: Justified

Tie, X., Geng, F., Guenther, A., Cao, J., Greenberg, J., Zhang, R., Apel, E., Li, G., Weinheimer, A., Chen, J., Cai, C.: Megacity impacts on regional ozone formation: Observations and WRF-Chem modeling for the MIRAGE-Shanghai field campaign, Atmos. Chem. Phys., 13, 5655–5669, https://doi.org/10.5194/acp-13-5655-2013, 2013.

USEPA: Guidance on the Use of Models and Other Analyses for Demonstrating Attainment of Air Quality Goals for Ozone, PM2.5 and Regional Haze, EPA-454/B-07e002. USEPA, 2007

von Schneidemesser, E., Coates, J., Denier van der Gon, H.A.C., Visschedijk, A.J.H., Butler, T.M.: Variation of the NMVOC speciation in the solvent sector and the sensitivity of modelled tropospheric ozone, Atmos. Environ., 135, 59–72, https://doi.org/10.1016/j.atmosenv.2016.03.057, 2016.

~~Walcek, C. J., Yuan, H.-H., Walcek, C. J. and Yuan, H.-H.: Calculated Influence of Temperature-Related Factors on Ozone Formation Rates in the Lower Troposphere, J. Appl. Meteorol., 34(5), 1056–1069, https://doi.org/10.1175/1520-0450(1995)034<1056:CIOTRF>2.0.CO;2, 1995.~~

Wang, S., Xing, J., Chatani, S., Hao, J., Klimont, Z., Cofala, J., Amann, M.: Verification of anthropogenic emissions of China by satellite and ground observations, Atmos. Environ., 45, 6347–6358, https://doi.org/10.1016/j.atmosenv.2011.08.054, 2011.

Wang, T.J., Lam, K.S., Xie, M., Wang, X.M., Carmichael, G., Li, Y.S.: Integrated studies of a photochemical smog episode in Hong Kong and regional transport in the Pearl River Delta of China, Tellus, Ser. B Chem. Phys. Meteorol., 58, 31–40, https://doi.org/10.1111/j.1600-0889.2005.00172.x, 2006.

Wang, T., Xue, L., Brimblecombe, P., Lam, Y. F., Li, L. and Zhang, L.: Ozone pollution in China: A review of concentrations, meteorological influences, chemical precursors, and effects, Sci. Total Environ., 575, 1582–1596, https://doi.org/10.1016/j.scitotenv.2016.10.081, 2017.

Wang, Y., Hu, B., Tang, G., Ji, D., Zhang, H., Bai, J., Wang, X., Wang, Y.: Characteristics of ozone and its precursors in Northern China: A comparative study of three sites, Atmos. Res., 132–133, 450–459, https://doi.org/10.1016/j.atmosres.2013.04.005, 2013.

Wang, Y.H., Hu, B., Ji, D.S., Liu, Z.R., Tang, G.Q., Xin, J.Y., Zhang, H.X., Song, T., Wang, L.L., Gao, W.K., Wang, X.K., Wang, Y.S.: Ozone weekend effects in the Beijing-Tianjin-Hebei metropolitan area, China, Atmos. Chem. Phys., 14, 2419–2429, https://doi.org/10.5194/acp-14-2419-2014, 2014.

~~Wilson, R.C., Fleming, Z.L., Monks, P.S., Clain, G., Henne, S., Konovalov, I.B., Szopa, S., Menut, L.: Have primary emission reduction measures reduced ozone across Europe? An analysis of European rural background ozone trends 1996-2005,~~Wu, K., Yang, X., Chen, D., Gu, S., Lu, Y., Jiang, Q., Wang, K., Ou, Y., Qian, Y., Shao, P.

Formatted: Font: (Asian) 等线, Font color: Auto

Formatted: Justified

and Lu, S. (2020). Estimation of biogenic VOC emissions and their corresponding impact on ozone and secondary organic aerosol formation in China. Atmos. Res. 231: 104656.

Wu, L., Shen, J.D., Feng, Y.C., Bi, X.H., Jiao, L. and Liu, S.X. (2014). Source apportionment of particulate matters in different size bins during hazy and non-hazy episodes in Hangzhou City. Res. Environ. Sci. 27: 373–381.

~~Atmos. Chem. Phys., 12, 437–454, https://doi.org/10.5194/acp-12-437-2012, 2012.~~

Xie, M., Zhu, K., Wang, T., Yang, H., Zhuang, B., Li, S., Li, M., Zhu, X., Ouyang, Y.: Application of photochemical indicators to evaluate ozone nonlinear chemistry and pollution control countermeasure in China, Atmos. Environ., 99, 466–473, https://doi.org/10.1016/j.atmosenv.2014.10.013, 2014.

Xue, L.K., Wang, T., Gao, J., Ding, A.J., Zhou, X.H., Blake, D.R., Wang, X.F., Saunders, S.M., Fan, S.J., Zuo, H.C., Zhang, Q.Z., Wang, W.X.: Ground-level ozone in four Chinese cities: Precursors, regional transport and heterogeneous processes, Atmos. Chem. Phys., 14, 13175–13188, https://doi.org/10.5194/acp-14-13175-2014, 2014.

Yan, R.S., Li, L., An, J.Y., Lu, Q., Wang, S., Zhu, Y., Jang, C.J. and Fu, J.S. (2016). Establishment and application of nonlinear response surface model of ozone in the Yangtze river delta region during summertime. Acta Sci. Circumstant. 36: 1383–1392.

Zhang, B.N., Kim Oanh, N.T.: Photochemical smog pollution in the Bangkok Metropolitan Region of Thailand in relation to O3 precursor concentrations and meteorological conditions, Atmos. Environ., 36, 4211–4222, https://doi.org/10.1016/S1352-2310(02)00348-5, 2002.

Zhang, G., Xu, H., Qi, B., Du, R., Gui, K., Wang, H., Jiang, W., Liang, L. and Xu, W. (2018). Characterization of atmospheric trace gases and particulate matter in Hangzhou, China. Atmos. Chem. Phys. 18: 1705–1728.

Zhang, H., Chen, G., Hu, J., Chen, S.H., Wiedinmyer, C., Kleeman, M., Ying, Q.: Evaluation of a seven-year air quality simulation using the Weather Research and Forecasting (WRF)/Community Multiscale Air Quality (CMAQ) models in the eastern United States, Sci. Total Environ., 473–474, 275–285, https://doi.org/10.1016/j.scitotenv.2013.11.121, 2014.

Zhi-zhen Ni, Kun Luo, Jun-xi Zhang, Rui Feng, He-xin Zheng, Hao-ran Zhu, Jing-fan Wang, Jian-ren Fan, Xiang Gao, Ke-fa Cen. Assessment of winter air pollution episodes using long-range transport modeling in Hangzhou, China, during World Internet Conference, 2015. Environmental Pollution 236 (2018) 550-561

Formatted: Font: (Asian) 等线, Font color: Auto

Formatted: Font: (Asian) 等线, Font color: Auto

Formatted: Justified

Formatted: Font: (Asian) 等线, Font color: Auto

Formatted: Justified

Formatted: Justified

Formatted: Font: (Asian) 等线, Font color: Auto

Formatted: Justified, Indent: Left: 0 cm, Hanging: 0.85 cm

Formatted: Font: (Asian) 等线, Font color: Auto

Page 1: [1] Style Definition	**kun luo**	**3/15/2020 1:24:00 PM**

定量线

Page 1: [2] Style Definition	**kun luo**	**3/15/2020 1:24:00 PM**

orange3

Page 1: [3] Style Definition	**kun luo**	**3/15/2020 1:24:00 PM**

背景对象: Font color: Black

Page 1: [4] Style Definition	**kun luo**	**3/15/2020 1:24:00 PM**

yellow3

Page 1: [5] Style Definition	**kun luo**	**3/15/2020 1:24:00 PM**

普通(网站)1: Font color: Black

Page 1: [6] Style Definition	**kun luo**	**3/15/2020 1:24:00 PM**

框架内容: Font color: Black

Page 1: [7] Style Definition	**kun luo**	**3/15/2020 1:24:00 PM**

表格内容: Font color: Black

Page 1: [8] Style Definition	**kun luo**	**3/15/2020 1:24:00 PM**

大标题 1

Page 1: [9] Style Definition	**kun luo**	**3/15/2020 1:24:00 PM**

lightblue3

Page 1: [10] Style Definition	**kun luo**	**3/15/2020 1:24:00 PM**

预格式化的文本: Font color: Black

Page 1: [11] Style Definition	**kun luo**	**3/15/2020 1:24:00 PM**

插图: Font color: Black, Don't suppress line numbers

Page 1: [12] Style Definition	**kun luo**	**3/15/2020 1:24:00 PM**

表格: Font color: Black, Don't suppress line numbers

Page 1: [13] Style Definition	**kun luo**	**3/15/2020 1:24:00 PM**

seetang3

Page 1: [14] Style Definition	**kun luo**	**3/15/2020 1:24:00 PM**

blue2

Page 1: [15] Style Definition	**kun luo**	**3/15/2020 1:24:00 PM**

orange2

Page 1: [16] Style Definition	**kun luo**	**3/15/2020 1:24:00 PM**

无填充的对象

Page 1: [17] Style Definition	**kun luo**	**3/15/2020 1:24:00 PM**

sun2

Page 1: [18] Style Definition	**kun luo**	**3/15/2020 1:24:00 PM**

gray1

Page 1: [19] Style Definition	kun luo	3/15/2020 1:24:00 PM

默认~LT~Hintergrund: Font color: Black

Page 1: [20] Style Definition	kun luo	3/15/2020 1:24:00 PM

gray3

Page 1: [21] Style Definition	kun luo	3/15/2020 1:24:00 PM

yellow2

Page 1: [22] Style Definition	kun luo	3/15/2020 1:24:00 PM

bw1

Page 1: [23] Style Definition	kun luo	3/15/2020 1:24:00 PM

sun3

Page 1: [24] Style Definition	kun luo	3/15/2020 1:24:00 PM

备注

Page 1: [25] Style Definition	kun luo	3/15/2020 1:24:00 PM

默认~LT~Gliederung 9

Page 1: [26] Style Definition	kun luo	3/15/2020 1:24:00 PM

turquoise2

Page 1: [27] Style Definition	kun luo	3/15/2020 1:24:00 PM

bw2

Page 1: [28] Style Definition	kun luo	3/15/2020 1:24:00 PM

默认~LT~Hintergrundobjekte: Font color: Black

Page 1: [29] Style Definition	kun luo	3/15/2020 1:24:00 PM

turquoise1

Page 1: [30] Style Definition	kun luo	3/15/2020 1:24:00 PM

大纲 8

Page 1: [31] Style Definition	kun luo	3/15/2020 1:24:00 PM

yellow1

Page 1: [32] Style Definition	kun luo	3/15/2020 1:24:00 PM

大纲 9

Page 1: [33] Style Definition	kun luo	3/15/2020 1:24:00 PM

sun1

Page 1: [34] Style Definition	kun luo	3/15/2020 1:24:00 PM

大纲 3

Page 1: [35] Style Definition	kun luo	3/15/2020 1:24:00 PM

默认~LT~Gliederung 4

Page 1: [36] Style Definition	kun luo	3/15/2020 1:24:00 PM

大纲 1

Page 1: [37] Style Definition **kun luo** **3/15/2020 1:24:00 PM**

默认~LT~Titel

Page 1: [38] Style Definition **kun luo** **3/15/2020 1:24:00 PM**

green3

Page 1: [39] Style Definition **kun luo** **3/15/2020 1:24:00 PM**

Fig.: Font color: Black, Don't suppress line numbers

Page 1: [40] Style Definition **kun luo** **3/15/2020 1:24:00 PM**

表格标题: Font color: Black

Page 1: [41] Style Definition **kun luo** **3/15/2020 1:24:00 PM**

bw3

Page 1: [42] Style Definition **kun luo** **3/15/2020 1:24:00 PM**

默认~LT~Gliederung 1

Page 1: [43] Style Definition **kun luo** **3/15/2020 1:24:00 PM**

默认~LT~Gliederung 6

Page 1: [44] Style Definition **kun luo** **3/15/2020 1:24:00 PM**

索引: Font color: Black, Don't suppress line numbers

Page 1: [45] Style Definition **kun luo** **3/15/2020 1:24:00 PM**

大纲 7

Page 1: [46] Style Definition **kun luo** **3/15/2020 1:24:00 PM**

无填充且无边框的对象

Page 1: [47] Style Definition **kun luo** **3/15/2020 1:24:00 PM**

gray2

Page 1: [48] Style Definition **kun luo** **3/15/2020 1:24:00 PM**

文本

Page 1: [49] Style Definition **kun luo** **3/15/2020 1:24:00 PM**

blue3

Page 1: [50] Style Definition **kun luo** **3/15/2020 1:24:00 PM**

arttitle: Font color: Black

Page 1: [51] Style Definition **kun luo** **3/15/2020 1:24:00 PM**

默认~LT~Gliederung 2

Page 1: [52] Style Definition **kun luo** **3/15/2020 1:24:00 PM**

orange1

Page 1: [53] Style Definition **kun luo** **3/15/2020 1:24:00 PM**

大标题 2

Page 1: [54] Style Definition **kun luo** **3/15/2020 1:24:00 PM**

默认~LT~Untertitel

Page 1: [55] Style Definition	kun luo	3/15/2020 1:24:00 PM

大纲 6

Page 1: [56] Style Definition	kun luo	3/15/2020 1:24:00 PM

Revision: Font color: Black

Page 1: [57] Style Definition	kun luo	3/15/2020 1:24:00 PM

默认~LT~Gliederung 7

Page 1: [58] Style Definition	kun luo	3/15/2020 1:24:00 PM

seetang2

Page 1: [59] Style Definition	kun luo	3/15/2020 1:24:00 PM

green2

Page 1: [60] Style Definition	kun luo	3/15/2020 1:24:00 PM

列表标题: Font color: Black

Page 1: [61] Style Definition	kun luo	3/15/2020 1:24:00 PM

earth1

Page 1: [62] Style Definition	kun luo	3/15/2020 1:24:00 PM

Normal (Web): Font color: Black

Page 1: [63] Style Definition	kun luo	3/15/2020 1:24:00 PM

标题 11: Font color: Black

Page 15: [64] Formatted	kun luo	3/15/2020 1:24:00 PM

Justified

Page 15: [65] Formatted	kun luo	3/15/2020 1:24:00 PM

First line: 0 ch

Page 15: [66] Formatted	kun luo	3/15/2020 1:24:00 PM

Font: (Asian) 等线

Page 15: [67] Formatted	kun luo	3/15/2020 1:24:00 PM

Font: (Asian) 等线, Font color: Auto

Page 15: [68] Formatted	kun luo	3/15/2020 1:24:00 PM

Font: (Asian) 等线

Page 15: [69] Formatted	kun luo	3/15/2020 1:24:00 PM

Font: (Asian) 等线, Font color: Auto

Page 15: [70] Formatted	kun luo	3/15/2020 1:24:00 PM

Font: (Asian) 等线, Font color: Auto

Page 15: [71] Formatted	kun luo	3/15/2020 1:24:00 PM

Font: (Asian) 等线, Not Bold, Font color: Auto

Page 15: [72] Formatted	kun luo	3/15/2020 1:24:00 PM

Font: (Asian) 等线, Font color: Auto

Page 15: [73] Formatted **kun luo** **3/15/2020 1:24:00 PM**

Font: (Asian) 等线, Font color: Auto

Page 15: [74] Formatted **kun luo** **3/15/2020 1:24:00 PM**

Font: (Asian) 等线

Page 15: [75] Formatted **kun luo** **3/15/2020 1:24:00 PM**

Font: (Asian) 等线, Font color: Auto

Page 15: [76] Formatted **kun luo** **3/15/2020 1:24:00 PM**

Font: (Asian) 等线

Page 15: [77] Formatted **kun luo** **3/15/2020 1:24:00 PM**

Font: (Asian) 等线, Font color: Auto

Page 15: [78] Formatted **kun luo** **3/15/2020 1:24:00 PM**

Font: (Asian) 等线

Page 15: [79] Formatted **kun luo** **3/15/2020 1:24:00 PM**

Font: (Asian) 等线, Font color: Auto

Page 15: [80] Formatted **kun luo** **3/15/2020 1:24:00 PM**

Font: (Asian) 等线

Page 15: [81] Formatted **kun luo** **3/15/2020 1:24:00 PM**

Font: (Asian) 等线, Font color: Auto

Page 15: [82] Formatted **kun luo** **3/15/2020 1:24:00 PM**

Font: (Asian) 等线, Font color: Auto

Page 15: [83] Formatted **kun luo** **3/15/2020 1:24:00 PM**

Font: (Asian) 等线, Font color: Auto

Page 15: [84] Formatted **kun luo** **3/15/2020 1:24:00 PM**

Font: (Asian) 等线, Font color: Auto

Page 15: [85] Formatted **kun luo** **3/15/2020 1:24:00 PM**

Font: (Asian) 等线

Page 15: [86] Formatted **kun luo** **3/15/2020 1:24:00 PM**

Font: (Asian) 等线, Font color: Auto

Page 15: [87] Formatted **kun luo** **3/15/2020 1:24:00 PM**

Font: (Asian) 等线

Page 15: [88] Formatted **kun luo** **3/15/2020 1:24:00 PM**

Font: (Asian) 等线, Font color: Auto

Page 15: [89] Formatted **kun luo** **3/15/2020 1:24:00 PM**

Font: (Asian) 等线, Font color: Auto

Page 15: [90] Formatted **kun luo** **3/15/2020 1:24:00 PM**

Font: (Asian) 等线, Font color: Auto

Page 15: [91] Formatted **kun luo** **3/15/2020 1:24:00 PM**

Font: (Asian) 等线

Page 15: [92] Formatted **kun luo** **3/15/2020 1:24:00 PM**

Font: (Asian) 等线, Font color: Auto

Page 15: [93] Formatted **kun luo** **3/15/2020 1:24:00 PM**

Font: (Asian) 等线, Font color: Auto

Page 15: [94] Formatted **kun luo** **3/15/2020 1:24:00 PM**

Font: (Asian) 等线

Page 15: [95] Formatted **kun luo** **3/15/2020 1:24:00 PM**

Font: (Asian) 等线, Font color: Auto

Page 15: [96] Formatted **kun luo** **3/15/2020 1:24:00 PM**

Font: (Asian) 等线

Page 15: [97] Formatted **kun luo** **3/15/2020 1:24:00 PM**

Font: (Asian) 等线, Font color: Auto

Page 15: [98] Formatted **kun luo** **3/15/2020 1:24:00 PM**

Font: (Asian) 等线, Font color: Auto

Page 15: [99] Formatted **kun luo** **3/15/2020 1:24:00 PM**

Font: (Asian) 等线

Page 15: [100] Formatted **kun luo** **3/15/2020 1:24:00 PM**

Font: (Asian) 等线, Font color: Auto

Page 15: [101] Formatted **kun luo** **3/15/2020 1:24:00 PM**

Font: (Asian) 等线, Font color: Auto

Page 15: [102] Formatted **kun luo** **3/15/2020 1:24:00 PM**

Font: (Asian) 等线

Page 15: [103] Formatted **kun luo** **3/15/2020 1:24:00 PM**

Font: (Asian) 等线, Font color: Auto

Page 15: [104] Formatted **kun luo** **3/15/2020 1:24:00 PM**

Font: (Asian) 等线

Page 15: [105] Formatted **kun luo** **3/15/2020 1:24:00 PM**

Font: (Asian) 等线, Font color: Auto

Page 15: [106] Formatted **kun luo** **3/15/2020 1:24:00 PM**

Font: (Asian) 等线, Font color: Auto

Page 15: [107] Formatted **kun luo** **3/15/2020 1:24:00 PM**

Font: (Asian) 等线, Font color: Auto

Page 15: [108] Formatted	kun luo	3/15/2020 1:24:00 PM

Font: (Asian) 等线

Page 15: [109] Formatted	kun luo	3/15/2020 1:24:00 PM

Font: (Asian) 等线, Font color: Auto

Page 15: [110] Formatted	kun luo	3/15/2020 1:24:00 PM

Font: (Asian) 等线

Page 15: [111] Formatted	kun luo	3/15/2020 1:24:00 PM

Font: (Asian) 等线, Font color: Auto

Page 20: [112] Formatted	kun luo	3/15/2020 1:24:00 PM

Default Paragraph Font, Font color: Auto

Page 20: [112] Formatted	kun luo	3/15/2020 1:24:00 PM

Default Paragraph Font, Font color: Auto

Page 20: [112] Formatted	kun luo	3/15/2020 1:24:00 PM

Default Paragraph Font, Font color: Auto

Page 20: [112] Formatted	kun luo	3/15/2020 1:24:00 PM

Default Paragraph Font, Font color: Auto

Page 20: [112] Formatted	kun luo	3/15/2020 1:24:00 PM

Default Paragraph Font, Font color: Auto

Page 20: [112] Formatted	kun luo	3/15/2020 1:24:00 PM

Default Paragraph Font, Font color: Auto

Page 20: [112] Formatted	kun luo	3/15/2020 1:24:00 PM

Default Paragraph Font, Font color: Auto

Page 20: [112] Formatted	kun luo	3/15/2020 1:24:00 PM

Default Paragraph Font, Font color: Auto

Page 20: [112] Formatted	kun luo	3/15/2020 1:24:00 PM

Default Paragraph Font, Font color: Auto

Page 20: [112] Formatted	kun luo	3/15/2020 1:24:00 PM

Default Paragraph Font, Font color: Auto

Page 20: [112] Formatted	kun luo	3/15/2020 1:24:00 PM

Default Paragraph Font, Font color: Auto

Page 20: [112] Formatted	kun luo	3/15/2020 1:24:00 PM

Default Paragraph Font, Font color: Auto

Page 20: [112] Formatted	kun luo	3/15/2020 1:24:00 PM

Default Paragraph Font, Font color: Auto

Page 20: [112] Formatted	kun luo	3/15/2020 1:24:00 PM

Default Paragraph Font, Font color: Auto

Page 20: [112] Formatted	kun luo	3/15/2020 1:24:00 PM

Default Paragraph Font, Font color: Auto

Page 20: [112] Formatted	kun luo	3/15/2020 1:24:00 PM

Default Paragraph Font, Font color: Auto

Page 20: [112] Formatted	kun luo	3/15/2020 1:24:00 PM

Default Paragraph Font, Font color: Auto

Page 20: [112] Formatted	kun luo	3/15/2020 1:24:00 PM

Default Paragraph Font, Font color: Auto

Page 20: [112] Formatted	kun luo	3/15/2020 1:24:00 PM

Default Paragraph Font, Font color: Auto

Page 20: [112] Formatted	kun luo	3/15/2020 1:24:00 PM

Default Paragraph Font, Font color: Auto

Page 20: [112] Formatted	kun luo	3/15/2020 1:24:00 PM

Default Paragraph Font, Font color: Auto

Page 20: [112] Formatted	kun luo	3/15/2020 1:24:00 PM

Default Paragraph Font, Font color: Auto

Page 20: [112] Formatted	kun luo	3/15/2020 1:24:00 PM

Default Paragraph Font, Font color: Auto

Page 20: [112] Formatted	kun luo	3/15/2020 1:24:00 PM

Default Paragraph Font, Font color: Auto

Page 20: [112] Formatted	kun luo	3/15/2020 1:24:00 PM

Default Paragraph Font, Font color: Auto

Page 20: [112] Formatted	kun luo	3/15/2020 1:24:00 PM

Default Paragraph Font, Font color: Auto

Page 20: [112] Formatted	kun luo	3/15/2020 1:24:00 PM

Default Paragraph Font, Font color: Auto

Page 20: [112] Formatted	kun luo	3/15/2020 1:24:00 PM

Default Paragraph Font, Font color: Auto

Page 20: [112] Formatted	kun luo	3/15/2020 1:24:00 PM

Default Paragraph Font, Font color: Auto

Page 20: [112] Formatted	kun luo	3/15/2020 1:24:00 PM

Default Paragraph Font, Font color: Auto

Page 20: [112] Formatted	kun luo	3/15/2020 1:24:00 PM

Default Paragraph Font, Font color: Auto

Page 20: [112] Formatted	kun luo	3/15/2020 1:24:00 PM

Default Paragraph Font, Font color: Auto

Page 20: [112] Formatted	kun luo	3/15/2020 1:24:00 PM

Default Paragraph Font, Font color: Auto

Page 20: [112] Formatted **kun luo** **3/15/2020 1:24:00 PM**

Default Paragraph Font, Font color: Auto

Page 20: [112] Formatted **kun luo** **3/15/2020 1:24:00 PM**

Default Paragraph Font, Font color: Auto

Page 20: [112] Formatted **kun luo** **3/15/2020 1:24:00 PM**

Default Paragraph Font, Font color: Auto

Page 20: [112] Formatted **kun luo** **3/15/2020 1:24:00 PM**

Default Paragraph Font, Font color: Auto

Page 20: [112] Formatted **kun luo** **3/15/2020 1:24:00 PM**

Default Paragraph Font, Font color: Auto

Page 20: [112] Formatted **kun luo** **3/15/2020 1:24:00 PM**

Default Paragraph Font, Font color: Auto

Page 20: [112] Formatted **kun luo** **3/15/2020 1:24:00 PM**

Default Paragraph Font, Font color: Auto

Page 20: [112] Formatted **kun luo** **3/15/2020 1:24:00 PM**

Default Paragraph Font, Font color: Auto

Page 20: [112] Formatted **kun luo** **3/15/2020 1:24:00 PM**

Default Paragraph Font, Font color: Auto

Page 20: [112] Formatted **kun luo** **3/15/2020 1:24:00 PM**

Default Paragraph Font, Font color: Auto

Page 20: [112] Formatted **kun luo** **3/15/2020 1:24:00 PM**

Default Paragraph Font, Font color: Auto

Page 20: [112] Formatted **kun luo** **3/15/2020 1:24:00 PM**

Default Paragraph Font, Font color: Auto

Page 20: [112] Formatted **kun luo** **3/15/2020 1:24:00 PM**

Default Paragraph Font, Font color: Auto

Page 20: [112] Formatted **kun luo** **3/15/2020 1:24:00 PM**

Default Paragraph Font, Font color: Auto

Page 20: [112] Formatted **kun luo** **3/15/2020 1:24:00 PM**

Default Paragraph Font, Font color: Auto

Page 27: [113] Formatted **kun luo** **3/15/2020 1:24:00 PM**

Font: (Asian) 等线, Font color: Auto

Page 27: [113] Formatted **kun luo** **3/15/2020 1:24:00 PM**

Font: (Asian) 等线, Font color: Auto

Page 27: [113] Formatted **kun luo** **3/15/2020 1:24:00 PM**

Font: (Asian) 等线, Font color: Auto

Page 27: [113] Formatted **kun luo** **3/15/2020 1:24:00 PM**

Font: (Asian) 等线, Font color: Auto

Page 27: [113] Formatted **kun luo** **3/15/2020 1:24:00 PM**

Font: (Asian) 等线, Font color: Auto

Page 27: [113] Formatted **kun luo** **3/15/2020 1:24:00 PM**

Font: (Asian) 等线, Font color: Auto

Page 27: [113] Formatted **kun luo** **3/15/2020 1:24:00 PM**

Font: (Asian) 等线, Font color: Auto

Page 27: [113] Formatted **kun luo** **3/15/2020 1:24:00 PM**

Font: (Asian) 等线, Font color: Auto

Page 27: [113] Formatted **kun luo** **3/15/2020 1:24:00 PM**

Font: (Asian) 等线, Font color: Auto

Page 27: [113] Formatted **kun luo** **3/15/2020 1:24:00 PM**

Font: (Asian) 等线, Font color: Auto

Page 27: [113] Formatted **kun luo** **3/15/2020 1:24:00 PM**

Font: (Asian) 等线, Font color: Auto

Page 27: [113] Formatted **kun luo** **3/15/2020 1:24:00 PM**

Font: (Asian) 等线, Font color: Auto

Page 27: [113] Formatted **kun luo** **3/15/2020 1:24:00 PM**

Font: (Asian) 等线, Font color: Auto

Page 27: [113] Formatted **kun luo** **3/15/2020 1:24:00 PM**

Font: (Asian) 等线, Font color: Auto

Page 27: [113] Formatted **kun luo** **3/15/2020 1:24:00 PM**

Font: (Asian) 等线, Font color: Auto

Page 27: [113] Formatted **kun luo** **3/15/2020 1:24:00 PM**

Font: (Asian) 等线, Font color: Auto

Page 27: [113] Formatted **kun luo** **3/15/2020 1:24:00 PM**

Font: (Asian) 等线, Font color: Auto

Page 27: [113] Formatted **kun luo** **3/15/2020 1:24:00 PM**

Font: (Asian) 等线, Font color: Auto

Page 27: [113] Formatted **kun luo** **3/15/2020 1:24:00 PM**

Font: (Asian) 等线, Font color: Auto

Page 27: [113] Formatted **kun luo** **3/15/2020 1:24:00 PM**

Font: (Asian) 等线, Font color: Auto

Page 27: [113] Formatted **kun luo** **3/15/2020 1:24:00 PM**

Font: (Asian) 等线, Font color: Auto

Page 27: [113] Formatted kun luo 3/15/2020 1:24:00 PM

Font: (Asian) 等线, Font color: Auto

Page 27: [113] Formatted kun luo 3/15/2020 1:24:00 PM

Font: (Asian) 等线, Font color: Auto

Page 27: [113] Formatted kun luo 3/15/2020 1:24:00 PM

Font: (Asian) 等线, Font color: Auto

Page 27: [113] Formatted kun luo 3/15/2020 1:24:00 PM

Font: (Asian) 等线, Font color: Auto

Page 27: [114] Formatted kun luo 3/15/2020 1:24:00 PM

Font: (Asian) 等线, Font color: Auto

Page 27: [114] Formatted kun luo 3/15/2020 1:24:00 PM

Font: (Asian) 等线, Font color: Auto

Page 27: [114] Formatted kun luo 3/15/2020 1:24:00 PM

Font: (Asian) 等线, Font color: Auto

Page 27: [114] Formatted kun luo 3/15/2020 1:24:00 PM

Font: (Asian) 等线, Font color: Auto

Page 27: [114] Formatted kun luo 3/15/2020 1:24:00 PM

Font: (Asian) 等线, Font color: Auto

Page 27: [114] Formatted kun luo 3/15/2020 1:24:00 PM

Font: (Asian) 等线, Font color: Auto

Page 27: [114] Formatted kun luo 3/15/2020 1:24:00 PM

Font: (Asian) 等线, Font color: Auto

Page 27: [114] Formatted kun luo 3/15/2020 1:24:00 PM

Font: (Asian) 等线, Font color: Auto

Page 27: [114] Formatted kun luo 3/15/2020 1:24:00 PM

Font: (Asian) 等线, Font color: Auto

Page 27: [114] Formatted kun luo 3/15/2020 1:24:00 PM

Font: (Asian) 等线, Font color: Auto

Page 27: [114] Formatted kun luo 3/15/2020 1:24:00 PM

Font: (Asian) 等线, Font color: Auto

Page 27: [114] Formatted kun luo 3/15/2020 1:24:00 PM

Font: (Asian) 等线, Font color: Auto

Page 27: [114] Formatted kun luo 3/15/2020 1:24:00 PM

Font: (Asian) 等线, Font color: Auto

Page 27: [114] Formatted kun luo 3/15/2020 1:24:00 PM

Font: (Asian) 等线, Font color: Auto

Page 27: [114] Formatted kun luo 3/15/2020 1:24:00 PM

Font: (Asian) 等线, Font color: Auto

Page 27: [114] Formatted kun luo 3/15/2020 1:24:00 PM

Font: (Asian) 等线, Font color: Auto

Page 27: [114] Formatted kun luo 3/15/2020 1:24:00 PM

Font: (Asian) 等线, Font color: Auto

Page 27: [114] Formatted kun luo 3/15/2020 1:24:00 PM

Font: (Asian) 等线, Font color: Auto

Page 27: [114] Formatted kun luo 3/15/2020 1:24:00 PM

Font: (Asian) 等线, Font color: Auto

Page 27: [114] Formatted kun luo 3/15/2020 1:24:00 PM

Font: (Asian) 等线, Font color: Auto

Page 27: [114] Formatted kun luo 3/15/2020 1:24:00 PM

Font: (Asian) 等线, Font color: Auto

Page 27: [114] Formatted kun luo 3/15/2020 1:24:00 PM

Font: (Asian) 等线, Font color: Auto

Page 27: [114] Formatted kun luo 3/15/2020 1:24:00 PM

Font: (Asian) 等线, Font color: Auto

Page 27: [114] Formatted kun luo 3/15/2020 1:24:00 PM

Font: (Asian) 等线, Font color: Auto

Page 27: [114] Formatted kun luo 3/15/2020 1:24:00 PM

Font: (Asian) 等线, Font color: Auto

Page 27: [114] Formatted kun luo 3/15/2020 1:24:00 PM

Font: (Asian) 等线, Font color: Auto

Page 27: [114] Formatted kun luo 3/15/2020 1:24:00 PM

Font: (Asian) 等线, Font color: Auto

Page 27: [114] Formatted kun luo 3/15/2020 1:24:00 PM

Font: (Asian) 等线, Font color: Auto

Page 27: [114] Formatted kun luo 3/15/2020 1:24:00 PM

Font: (Asian) 等线, Font color: Auto

Page 27: [114] Formatted kun luo 3/15/2020 1:24:00 PM

Font: (Asian) 等线, Font color: Auto

Page 27: [114] Formatted kun luo 3/15/2020 1:24:00 PM

Font: (Asian) 等线, Font color: Auto

Page 27: [114] Formatted **kun luo** **3/15/2020 1:24:00 PM**

Font: (Asian) 等线, Font color: Auto

Page 27: [114] Formatted **kun luo** **3/15/2020 1:24:00 PM**

Font: (Asian) 等线, Font color: Auto

Page 27: [114] Formatted **kun luo** **3/15/2020 1:24:00 PM**

Font: (Asian) 等线, Font color: Auto

Page 27: [114] Formatted **kun luo** **3/15/2020 1:24:00 PM**

Font: (Asian) 等线, Font color: Auto

Page 27: [114] Formatted **kun luo** **3/15/2020 1:24:00 PM**

Font: (Asian) 等线, Font color: Auto

Page 27: [114] Formatted **kun luo** **3/15/2020 1:24:00 PM**

Font: (Asian) 等线, Font color: Auto

Page 27: [114] Formatted **kun luo** **3/15/2020 1:24:00 PM**

Font: (Asian) 等线, Font color: Auto

Page 27: [114] Formatted **kun luo** **3/15/2020 1:24:00 PM**

Font: (Asian) 等线, Font color: Auto

Page 27: [114] Formatted **kun luo** **3/15/2020 1:24:00 PM**

Font: (Asian) 等线, Font color: Auto

Page 27: [114] Formatted **kun luo** **3/15/2020 1:24:00 PM**

Font: (Asian) 等线, Font color: Auto

Page 27: [114] Formatted **kun luo** **3/15/2020 1:24:00 PM**

Font: (Asian) 等线, Font color: Auto

Page 27: [114] Formatted **kun luo** **3/15/2020 1:24:00 PM**

Font: (Asian) 等线, Font color: Auto

Page 27: [114] Formatted **kun luo** **3/15/2020 1:24:00 PM**

Font: (Asian) 等线, Font color: Auto

Page 27: [114] Formatted **kun luo** **3/15/2020 1:24:00 PM**

Font: (Asian) 等线, Font color: Auto